T. R.
KAHRAMANMARAS SUTCU IMAM UNIVERSITY
GRADUATE SCHOOL OF NATURAL AND APPLIED SCIENCES

ASSESSMENT THE IMPACT OF URBAN EXPANSION ON LAND SURFACE TEMPERATURE USING GIS AND RS TECHNIQUES FROM THE CASE OF SORAN-ERBIL, IRAQ

CHIYA SAMI SULAUIMAN

MASTER'S THESIS
DEPARTMENT OF BIOENGINEERING AND SCIENCES

KAHRAMANMARAŞ - TURKEY 2018

T.R.

KAHRAMANMARAS SUTCU IMAM UNIVERSITY

GRADUATE SCHOOL OF NATURAL AND APPLIED SCIENCES

ASSESSMENT THE IMPACT OF URBAN EXPANSION ON LAND SURFACE TEMPERATURE USING GIS AND RS TECHNIQUES FROM THE CASE OF SORAN-ERBIL, IRAQ

CHIYA SAMI SULAIMAN

A thesis submitted in partial fulfillment of the requirements for the degree of Master of Science in Bioengineering and Sciences

KAHRAMANMARAŞ -TURKEY 2018

The current M.Sc. thesis is entitled " ASSESSMENT THE IMPACT OF URBAN EXPANSION ON LAND SURFACE TEMPERATURE USING GIS AND RS TECHNIQUES FROM THE CASE OF SORAN-ERBIL, IRAQ" by Chiya Sami Sulaiman, who is a student at Department of Bioengineering and Sciences, Graduate School of Natural and Applied Sciences, Kahramanmaraş Sütçü Imam University, was certified by all the majority jury members, whose signatures are given below at the date of 04.04.2018.

Assoc. Prof. Dr. Çağatay TANRIVERDİ (Supervisor) …….
Department of Bio systems engineering
Kahramanmaraş Sütçü İmam University

Dr. Kamaran Wali MAHMOOD (CO- Supervisor) …….
Department of Geography
Soran University

Prof. Dr. Hasan DEĞĞRMENCĠ (Member) .....…….....
Department of Bio systems engineering
Kahramanmaraş Sütçü İmam University

Prof. Dr. Atılgan ATILGAN (Member) …….
Department of Agriculture Structure and Irrigation
Süleyman Demirel University

Assoc. Dr. Hasan SERİN (Member) …….
Department of Forest Industry Engineering
Kahramanmaraş Sütçü Ġmam University

I approve that the above signatures related to the members.
Assoc. Prof. Dr. MUSTAFA ŞEKKELI
…….
Director of Graduate School of Natural and Applied Sciences
Kahramanmaraş Sütçü İmam University

DECLARATION

I declare and guarantee that all information in this document has been obtained and presented in accordance with academic rules and ethical conduct. Based on these rules and conduct, I have fully cited and referenced all materials and results that are not original to this work.

CHIYA SAMI SULAIMAN

IRAK SORAN-ERBİL, BÖLGESİ'NDE COĞRAFİ BİLGİ SİSTEMLERİ VE UZAKTAN ALGILAMA TEKNİKLERİNİ KULLANARAK KENTSEL BÜYÜMENİN KENT YÜZEY SICAKLIĞI ÜZERİNE ETKİSİNİN DEĞERLENDİRİLMESİ

(YÜKSEK LİSANS TEZİ)

CHIYA SAMI SULAIMAN

ÖZET

Bu çalışmanın amacı arazi yüzey sıcaklığı (LST) derecesi kentsel büyüme üzerine yarattığı etkiyi belirlemektir.Çalışme Soran- Erbil, Irak bölgesi değerleri için yapılmıştır. 1995 ve 2011 yıllarına ait Landsat-5 TM görüntüleri ve GIS tekniği kullanılarak LST değerleri belirlenmiştir. 1995 ve 2011 yıllarına ait LST'nin mekansal dağılımı sonuçları karşılaştırılmadan önce, şehir içindeki ve dışındaki yeni kurulan bölgeler araştırılmıştır. Bu nedenle, çeşitli arazi örtüsü tiplerinin sınıflandırılmasında, arazi örtüsü sınıflarındaki potansiyel değişikliklerin tespit edilmesi amacıyla denetimli sınıflandırma işlemi yapılmıştır. LST verilerinin ölçümü Radyasyon Transferi Denklemi (RTE) aleti kullanılarak toplenmştır. Bulgulara göre, Soran-Erbil'i, hızlı kentsel genişlemesi, toprak örtüsü niteliğinin LST sonuçları üzerinde negetif ve geniş kapsamlı sonuçları olan bir trendi karakterize etmektedir.

Kentsel genişleme uygulamasında 1995 yılı için % 44, 97 oranından 2011 yılında ise % 57, 26'ya yükselirken, söz konusu arazi örtüsü sınıflarının da etkilendiği görülmüştür. Örneğin, kentsel genişlemenin, bitki örtüsündeki 1995'te %17.46'dan 2011'de % 11,8'e önemli bir düşüşe neden olduğu görülmektedir. LST değerlerinin mekânsal dağılımı, kentsel merkezine yakın olan yeni bölgelerdeki, ilçelerin eski ilçelere kıyasla en yüksek değerlere sahip olduğunu göstermektedir. Yeni inşa edilen ilçelerin şehir dışında ya da çevresinde daha yoğun olduğu göz önüne alındığında, olasılık, LST değerlerinin, iki yıl boyunca kentsel bölge dışındaki bölgelerde, 1995da 40 ºC ve 40 ºC üstü olduğu şeklindedir. LST değerlerinde varyasyonların da arazi örtüsünün türüne, sınıfına ve niteliğine bağlı olduğu bulunmuştur. Spesifik arazi örtüsü türleri ile ilgili olarak, 1995 yılında 34 ºC ve 2011, yıllında 39.5 ºC olduğu en düşük LST değerlerinin ise bitki örtüsü ve su yüzeylerinin sahip olduğu belirlenmiştir. Diğer arazi örtüsü kategorilerinin daha yüksek LST değerlerine sahip olduğu görülmüştür. Dikkat edilmesi gereken husus, 2011 yılının 1995 yılı sonuçlarıyla

karşılaştırıldığında, hem en düşük sıcaklığa sahip hem de en yüksek sıcaklığa sahip arazi örtüsü tiplerinde, LST değerlerinde önemli bir artışın olduğu görülmüştür. Ayrıca bu çalışmada NDVI ile LST değerleri arasındaki ilişki incelenmiştir. Sonuçta, nitelikler ve değişkenler arasında güçlü bir negatif korelasyon bulunduğu belirlenmiştir. Bu değerler, 1995 ve 2011 için sırasıyla -0.81 ve -0.77 dir.

Özetle, bu çalışmada, Soran-Erbil bölgelesinde LST değerlerine kentsel genişleme etkisini araştıran uzaktan algılama teknikleri ile elde edilen sonuçların CBS'ne entegrasyonun geçerliği ve güvenilir sonuçlar elde edildiği görülmüştür. Sonuç olarak, bu çalışme sonuçların çevreci olarak şehir planlamasına en uygun ve etkili yaklaşımları gösteren grupları belirlerken son derece faydalı olacağı, sürdürülebilir kalkınmanın arzulanan durumuna doğru çaba sarf etmeleridir.

Anahtar kelimeler: Arazi kullanımı/arazi örtüsü, LST, Termal ku şak, Landsat, GIS.

Kahramanmaras Sütçü İmam Üniversitesi

Fen Bilimleri Enstitüsü

Biyomühendislik ve Bilimleri Anabilim Dalı, Nisan / 2018

Danışman: Doç. Dr. Çağatay TANRIVERDI

Sayfa numarası: 82

ASSESSMENT THE IMPACT OF URBAN EXPANSION ON LAND SURFACE TEMPERATURE USING GIS AND RS TECHNIQUES FROM THE CASE OF SORAN-ERBIL, IRAQ (M.Sc. THESIS)

CHIYA SAMI SULAIMAN

ABSTRACT

In this study, the main aim was to determine the impact posed by urban expansion of the degree of land surface temperature (LST). The specific focus was in the context of Soran-Erbil, Iraq. To determine the resultant LST values, images for the years 1995 and 2011 were used in terms of Landsat-5 TM imagery and the GIS technique. The spatial distribution of LST was also investigated in terms of the newly built districts within and outside the city before comparing the respective outcomes for the years 1995 and 2011. Thus, the classification of various types of land cover was achieved via the supervised classification process with the aim of fostering detections of potential changes in the respective classes of land cover. The retrieval of LST data was also achieved via the use of the Radiative Transfer Equation (RTE). From the findings, a fast-paced state of urban expansion characterizes Soran-Erbil, a trend that has had far-reaching consequences on the nature of the land cover that, in turn, has had a trickle-down effect on LST value outcomes.

With the practice of urban expansion increasing the coverage from 44.97 % for the year 1995 to 57.26 % for the year 2011, the respective classes of land cover were also seen to be affected. For example, urban expansion is seen to account for the significant decline in vegetation cover from 17.46 % in 1995 to 11.8 % in 2011. In relation to the newly built districts, the spatial distribution of LST value outcomes indicated that those districts that were close to the urban zone had the highest values when compared to the older districts. Given that the newly built districts were more concentrated outside or around the city, the eventuality was that LST values were higher in regions outside the urban zone for the two years which is 40 ºC in 1995 and 44 ºC. Variations in LST values were also found to be dependent on the type, class or nature of the land cover. Regarding these specific types of land cover in 1995 is 34 ºC and 2011 is 39.5 ºC, vegetation and water surfaces were found to exhibit the lowest LST values. The other categories of land cover revealed higher LST values. Imperative to note is that both the land cover types with the lowest temperature and those with the highest temperature saw the year 2011 witness a significant increase in LST values when compared to the outcomes for the year 1995. The nature of the relationship

between NDVI values and LST values was also examined in this study. From the outcomes, it was established that a strongly negative correlation exists between these attributes or variables. Precisely, this was -0.81 and -0.77 for 1995 and 2011 respectively.

In summary, this study revealed that the integration of the GIS data into the outcomes obtained via RS techniques fosters outcome validity and reliability when investigating the impact of urban expansion on LST values in zones such as Soran-Erbil. The eventuality is that such outcomes are highly beneficial because they inform groups such as environmentalists regarding the most appropriate and/or effective approaches to urban planning while striving towards the desirable state of sustainable development.

Key words: Land use/land cover, LST, Thermal band, Landsat, GIS, RS.

Kahramanmaraş Sütçü İmam University

Graduate School of Natural and Applied Sciences

Department of Bioengineering and Sciences, April, 2018

Supervisor: Assoc.Prof.Dr.Çağatay TANRIVERDİ

Page count: 82

ACKNOWLEDGMENTS

I want to express my best thanks to a special gratitude to my supervisor, Assoc. Prof.Dr. Çağatay TANRIVERDİ who has invested his full effort in guiding me to finish my research. I would also like to my Co-supervisor Dr. Kamaran Wali MAHMOOD for his surveillance.

I would like to thank everyone who has given me support and encouragement over the year in completing this dissertation

I am very grateful and thankful to my father, mother, my wife, my sisters, and my brother for their support during my study and an impeccable understanding allowed me to accomplish this thesis. I would like to express my deepest appreciation to my friends and all those who provided me with assistance to complete this research. Finally, I wish to thank my best friends, Fırat Arslan, Engin Gönen Diyar Jamal, Jawhar Kareem, Ardalan Mohammad, Hedi jamal, Daban kadhim, for their support and encouragement throughout my study.

Chiya Sami Sulaiman BAG

1

TABLE OF CONTENTS

Page No.

LIST OF TABLES

Page No

LIST OF FIGURES

Page No

i

THE LIST OF SYMBOLOS AND ABBEVIATIONS

DG:	Digital Numbers
GCM:	Global circulation models
GIS:	Geographic Information Systems
HA:	Hectare
LST:	Land Surface Temperature
LU/LC:	Land Use / Land Cover
NDVI:	Normalized Different Vegetation Index
RS:	Remote Sensing
RTE:	Radiative Transfer Equation
TC:	Tasselled Cap
TM:	Thematic Mapper
TOA:	Top-of-atmosphere
UHI:	Urban Heat Island
USGS:	United States Geological Survey
UTM:	Universal Transverse Mercator Coordinate System
WGS:	World Geodetic System

1. INTRODUCTION

Recent times have witnessed the aspect of urban expansion emerge as a subject that is not only debatable but also attracted the attention of scientific groups and academic professionals. Specifically, expansion in this context entails the process of covering expansive tracts of land by erecting buildings. A major adversity associated with situations where the erecting of these buildings has been unplanned has been documented to lie in the negative attribute of untidiness. Similarly, the decision to conduct expansions of urban areas has been considered unacceptable by environmentalists due to the lacking state of natural resource management and a compromised state of air quality. Indeed, it can be inferred that urban expansion leads to significant alterations in the nature of cover in the natural environment or land, proceeding to affect man-made or built environments; yet the latter play the critical role of serving the needs of humans. According to Mallick et al. (2008), built environments pose the negative effect on arable land and yield alterations in the physical outlook of components on land surfaces; including soil moisture and the land surface's thermal capacity. Hence, it can be inferred that urban expansion remains associated with alternations in the natural environment, extending similar effects to the sub-urban zones. The eventuality is that urban expansion is that which yields negative outcomes on the natural environment; fostering direct and indirect impacts on aspects such as life quality, human activities, health, and mortality rates in urban settings (Gartland, 2008; Bhatta, 2010; Saleh, 2011). Generally, with new types of networks, it is difficult to experiment. Because new types of networks use several addressing schemes and include other non-standard aspects. It is difficult to incorporate these modifications into existing networks. In SDN, using a controller, new ideas and inventions can be experimented in different network settings.

In the urban set-up, it has been observed that urbanization causes changes in the atmosphere's concentration, alterations in physical properties, and the spread of pollution (air, water, and soil). The tertiary impact of these adversities has been the formation of urban heat islands. In a study by (Oke, 1988), it was observed that urban heat islands refer to man-made regions whose temperatures are higher than those of the surrounding. Hence, urban heat island intensity aids in determining the degree of heat in urban areas and entails the difference between the background rural temperature and the maximum urban temperature (Mills, 2007). From the documentation, it is evident that the formation of urban heat islands results when the urban areas' land surfaces absorb heat from different sources, including the

sun. The resultant characteristic constitutes reduced ventilation due to compromised degrees of air quality and the consumption of concentrated energy. This difference between the urban heat island and the rest of the surrounding has been observed to be pronounced during winter and summer, in the presence of weaker winds, and during the night (Mills, 2007).

Two forms of heat islands have been documented. On the one hand, surface urban heat islands are measured via remote sensing and form at the surface. On the other hand, atmospheric heat islands are measured by mobile transverses and weather stations and form in the air (Mills, 2007). Notably, specific adverse effects accruing from the formation of urban heat islands include increased mortality rates due to poor health, impaired levels of water quality, the emission of greenhouse gases and related air pollution, a rise in energy consumption, and deteriorations in the degree of the living environment's quality (Rizwan et al., 2008; Akbari et al., 2008). The eventuality has been a drawn attention of urban climate engineers and researchers due to the economic impact and adverse environment effects posed by urban heat islands. Specific emphasis has been on the need to determine the degree of the heat and engage in interventions or mitigation measures poised to counter the resultant challenges (Arnfield, 2003; Grimond, 2005; Rizwan et al., 2008). This study seeks to determine the impact posed by built environments (via urban expansion) on urban heat islands. Specifically, the study will investigate the manner in which temperature son urban land surfaces are distributed in the context of Soran-Erbil, Iraq.

According to Voogt and Oke (2003), land surface temperature (LST) poses a direct impact on the formation of urban heat islands (UHIS) and their accompanying effect of environmental alteration. For example, LST affects the nature of environmental and atmospheric issues such as the exchange of sensible latent and surface heat flux in the environment (Prigent et al., 2003). Hence, it is evident that LST plays a critical role and predictor among studies that focus on global and regional climate changes, important in conducting estimations of the level of balance in the surface energy (Jin and Dickinson, 1999; Sun and Pinker 2003; Oluesyi et al., 2011). Similarly, LST is important because it aids in obtaining data regarding different land surfaces' physical properties. As concurred by (Wan and Dozier, 1996; Kerr et al., 2005), estimating the level of LST is crucial in achieving various global circulation models (GCM), hydrological, geological, climatic, and vegetation monitoring models.

Therefore, a majority of the international and national firms have concentrated on the collection and monitoring of data regarding LST to predict future outcomes in built environments arising from urban expansion. For example, remote sensing adoption and application has been witnessed at the Intergovernmental Panel on Climate Change while seeking to determine possibilities of global warming. It has been used very much in recent years for agricultural purposes (Tanriverdi, 2010). Similarly, data from remotely sensed thermal infrared has played an important role of determining the adversities of urban heat islands while additional data in relation to thermal infrared has been obtained via airborne sensors and satellites. It is worth highlighting that airborne sensors include TIMS, ASTER, MODIS, AVHRR, and Landsat TM/ETM+ (Mather, 2004). Notably, thermal infrared data has been used for purposes of revealing the degree of LST as well as the determination of the nature of emissivity in different types of land cover. The criticality of such outcomes is that LST predicts the nature of energy exchange and surface radiation in a given environment, including urban zones that have undergone expansion. As observed by and (Qin, 2001; Zhang, 2006), surface heat fluxes play the important role of governing LST distribution, with urbanization determining the level of these surface heat fluxes.

Indeed, this investigation was in the form of an LST-related study seeking to understand the impact of urban expansion in the context of Soran-Erbil, Iraq. The rationale for conducting the study was informed by the vast or rapid expansion of the region, with the impact of this expansion on the region's degree of land surface temperature remaining dire. In addition, the study was motivated by scanty information regarding approaches that have employed remote sensing and geographical information systems to unearth the resultant impact of urban expansion in Soran-Erbil on the resultant LST. It is further notable that the study was motivated by the threat of urban expansion in relation to adversities such as the recurrence of sand storms, desertification, and drought ─ especially during the year's hottest months.

Various benefits are predicted to arise from the perceived findings, data collection, analysis, interpretation, discussion, and recommendations. For example, the outcomes would inform the need for regional and local planning in relation to Soran-Erbil. With remote sensing and geographical information systems (GIS) employed, the study would foster the detection and monitoring of changes in the region's environment to inform decision-making about problems that the surrounding community could encounter due to continued urban

expansion. In turn, advance mitigation measures or timely interventions might be attracted and save the economy of the region via improved environmental quality and save the lives of individuals due to the curbing of health adversities associated with urban expansion and the resultant environmental compromise. The following section provides the review of literature regarding some of the past scholarly contributions that have examined this subject from various contexts. Indeed, the section is poised to form a foundation from which the methodology will be described and data collected towards inference making and determine whether parallels can be drawn between this study's findings and the existing literature or significant differences in outcomes are evident.

2. LITERATURE REVIEW

Several explorations have shown that the use of satellites and the thermal band have reclaimed land surface temperatures (LST) associated with the urban environments. A Landsat thermal band is among the most extensively used means of gathering data in the field. This chapter discusses the major applicable work in consideration to those that have already used Landsat pictures to reclaim LST. It gives the impression of the appraised research that has been evidenced by several explorations that mostly concentrated on outlining the correlation between the cover of the land classes and LST.

This aspect was brought forward by the difference observed between the diverse thermal physical appearances of the land covers surveyed, revealing dissimilarities in LST. For example, (Honjo et al., 2004), concentrated on the influence of green spaces on LST in the circumstances that entailed Iraq and Japan. The customary classification technique with a Landsat-5 TM and ETM+7 was castoff to recognize and make out different land covers in the research region. The exploration used size, shape, and parts of green space as gauges for appraising the importance of green areas with respect to LST. As a result, this study discovered that the size and shape of the green areas in Iraq had a substantial role in decreasing overall LST. An equivalent study was prepared by Rajeshwari and Mani (2014), who used Landsat-8 thermal bands to estimate the effect of vegetation on the LST of the Dindigul District, Tamil Nadu, India. In this study, a split window algorithm was used to retrieve LST. For this reason, they used NDVI to assess the emissivity over the study area. As in the preceding study, the result exposed that the uppermost LST was discovered over desolate land, and the lowermost LST was revealed over vegetated terrestrial cover.

Kwarteng and Small (2005), associated the dualistic metropolises within binary dissimilar topographical places. The paramount one was within Kuwait City, Arabian bare land region, while subsequent one was the City of New York. They both used Landsat ETM+ in addition to the temperature equation of satellite brightness to discover the LST. The fallouts emphasized evidently that, in the City of Kuwait, LST was inferior compared to the neigh boring desert areas because of the deficiency of dominant foliage in the adjacent zones. As a result, nearly all of the land cover in the nearby areas conveyed higher solar energy than in the urban background attributable to lack of evaporation process that indicates varying the humidity heat. Contrary, in the city of New York, LST was sophisticated within the developed zones compared to the contiguous regions due to the density of the vegetation

that surrounded the city. Besides, it played a major part in the preservation of the air through evaporating and received solar radiation. The study's outcomes exhibited that terrestrial environments help the process of recording level LST in city areas instead of the surrounding places. For example, Kuwait City that is situated in a desert area recorded a lower LST compared to the surrounding parts.

In the same way, an identical study was carried out by (Frey et al., 2005), who designated two coastal conurbations in the United Arab Emirates (Dubai and Abu Dhabi). The two cities are found in a dry desert surroundings and their main reason for the investigation was to scrutinize the part of metropolitan capacities in a dry surroundings within relation to the production Urban Cool Island (UCI). The domino effect clearly pointed out that the two cities were producing a daily UCI because of the albedo all over the place in both cities (with respect to dry land that was higher compared to the urban areas). The observation showed that the former surface had high temperature.

In addition, Habib (2007), used Landsat-5 TM to salvage LST in the Saudi Arabian city of Dammam. The consequences of the study exhibited two important arguments. The first point revealed that, it was discovered that well-planned metropolitan areas controlled and reduced the LST. For instance, it is widely acknowledged in the literature that the Central Business District (CBD) that was the main in the city, was alleged to have an excessive LST. On the other hand, Dammam's CBD documented a lower LST compared to the neigh boring districts because of partaking a large quantity of greenery that facilitated the lessening of LST compared to supplementary parts of the city. The second point of the exploration recommended and encouraged the people to proceed with their buildings and construction in the bare terrestrial at similar time as consuming adequate quantities of green space to lessening LST.

In addition, the role of evaporation in the course of the spatial delivery of LST has been premeditated. It was done by (Ahmed et al., 2005), in the Gezira area of Sudan's desert. They took into consideration the aspect of SEBAL algorithm in order to work out the rate vaporization. The analysis discovered that dehydration was an imperative consideration while decreasing LST within the region and outcomes sustained the inkling. Back in 2001, the proportion of vaporization was 4.36% over the stagnated areas, besides, 300.7 K degree of the LST. Nevertheless, on unproductive terrestrial, within the very year, the LST recorded 313.6 K through a 0.0 proportion of evaporation. It had an apparent impact in terms of

vegetation decreasing LST by producing evaporation. Moreover, (Bounoua et al., 2009), castoff Landsat ETM+ statistics to pinpoint the influence of an LST on the dynamic forces of moving liquid, and the stability of carbon as well as external dynamism in the semi-arid section of the residential area of Oran City in Algeria. The fallouts revealed and evidenced, it was likely for an inner-city part to perform a progressive part in declining LST in parched along with semi-arid regions. As exposed by the investigation, the metropolitan development of the city in Oran had a fragile influence in terms of turning out an isle of heat in the area. In addition, the domino effect exhibited that the dynamics of the pointers were affected in a great way by the kind of cover in the piece of land and the recognized shrubbery. The major important indicator was the decrease of LST besides carbon uptake. Accordingly, the study acclaimed the ongoing procedure of creating in this area, in conjunction with establishing and developing plants that were moderately significant in dropping LST and delivering an improved background of persons existing in the city.

Zhang and Ban (2011), were using Landsat TM to explore the LST of Beijing. They tried to examine the impact of urban development on LST at the heart of the years 2004 - 2009. NDVI was used as a consideration to extract surface emissivity. They discovered a non-equal as well as non-concentric spatial outline dissemination of LST amongst the city districts. Moreover, LST in Beijing's city was different in various regions because several outcomes recorded high LST whereas on the other side others recorded low LST. Nevertheless, all of these constituencies were inside the conurbation and not in the suburban areas. These striking dissimilarities between the districts were associated with green spaces as well as thermal characteristics. Additionally, the investigation employed an association examination between LST and NDVI, in 2004 - 2009. The fallouts were a negative connection of -0.732 and -0.751 and in that order. In the same way, Saleh (2011), premeditated Baghdad, which is Iraq's capital city. He concentrated mostly on the influence of the development of Baghdad City on LST in the middle of 1961 to 2001. A customary arrangement technique was used based on high determination IKONOS statistics. The investigation area alienated keen on seven diverse programs. A traditional simple calculation was used to change the satellite numerical numbers to satellite illumination temperatures. The research pointed out that the LST improved between the acknowledged years in line with the modification of terrestrial vegetation cover relate to the human-made land cover. For instance, in the orchard region, the LST stood at approximately 33.37 ºC. Nonetheless, on unproductive domains and built up zones, it stayed around 49.01 ºC and 46.97 ºC

correspondingly. As a result, the exploration discovered an enlargement in the city of Baghdad instigated a decline in shrubbery cover as well as triggering LST towards intensification, particularly within parts that did not have plants.

Likewise in Vijayawada, India, (Kumar et al., 2012).The study was carried out on the impact of diverse terrestrial concealment forms on the LST. The use of Landsat ETM+ was instigated as the main statistics, while investigators used satellite brightness heats retrieved from the thermal band. Additionally, NDVI was used for binary determinations: in the first place, the recognition of an influence of foliage on LST; while the second, to repossess acreage superficial emissivity on the basis standards of NDVI. An outcome established relationship concerning LST and NDVI to be approximately -0.79. Furthermore, with respect to this research's outcomes, it looks as if the zones of vegetation had an influential role to play in reducing and controlling LST in that they discovered the highest LST to be noted down on the built-up land 320 K and the lowermost LST recorded in zones of greenery, which was about 299 K.

A long way from examining besides discovering a correlation between land cover and LST (Oluseyi et al., 2011), used Landsat statistics in the recognition of causes of mosquito infiltration in Nigeria. The principal aim of the exploration was to benefit the individuals in the region to overwhelmed delinquent that they encountered from the mosquitoes conveying sickness. Consequently, two Landsat images were used between the years 1995 and 2006. In general, the investigators watched for variations in using of lands as well as the land cover, and the effect on LST. Accordingly, they were competent to recognize the warmest places in the city and related the information to mosquito invasion. The consequences established that alteration in covering of land and terrestrial use brought changes in LST and, therefore, those zones that recorded large LST on the built-up area were infected with mosquitoes. Apparently, the contradictory was grasped with standard LST in the bodies of land covered by vegetation and water.

Besides, Oguz (2013), endeavoured to build a computer-based software package to compute LST in a straightforward and quick way related to other methods. He organized a program based on C++ using a single-channel algorithm to salvage LST using Landsat thermal bands. It is significant to say that this tactic is one of the most precise methods for calculating LST.

It is due to the usage of various variables in the course of computing LST. To summarize, it can be assumed that there were certain goals amongst the literature that were cast-off extensively and engaged in an investigation on LST within metropolitan parts. The purposes included the influence of inner city of LST, the correlation in LST in diverse categories of terrestrial asylum, as well as the essence of greenery among others. In addition, various pieces of literature gave similar outcomes concerning the urban areas and LST. They discovered that LST was higher in the city regions compared to the neigh boring areas. However, as revealed in the works by (Ahmed et al., 2005; Kwarteng and Small, 2005; Habib, 2007; Bounoua et al., 2009), particular literature showed a contradictory outcome. The specification in the municipal regions, LST, was considerably lesser compared to rural parts because of climatic besides geographical conditions of those regions in the deserting addition, there was a kind of arrangement through the collected works concerning significant role of greenery zones in scheming and dropping LST.

Consequently, through an examination designated in different landmark documents on LST using the remote sensing statistics and its related procedures, it can be anticipated that common objectives within the literature existed, used widely and were employed in the exploration of land surface temperature using Landsat data. Nevertheless, the study clearly acknowledged two definite research differences within the literature. The first gaps entail the differences in the investigation regarding the systems used for salvaging LST. Therefore, the exploration has tried to close the gap by the utilization of a correct method to compute LST on Landsat Thermal band basis. The technique works on various parameters that help to calculate LST in a proper way. Secondly, as showed openly in the literature, specific thermal characteristic for every type of land cover was observed. However, it gives the impression that there were almost no explorations on longitudinal circulation of LST in the urban areas and the surrounding areas. Therefore, this analysis attempted to explore the three-dimensional dissemination of the LST within Soran City and its adjoining region, and concentrated on an association in the middle of LST and diverse nature of land cover, in particular on the full land and vegetation. It was carried out by engaging the Radiative Transfer Equation (RTE) through a Landsat-5 TM thermal band, along with incorporating with a geographical Information system.

Mahmood (2017), the wonder of urban expansion is one of the major difficulties fronting the authorities in responsibility of the administration and urban planning, especially

subsequently the growths of transport technology. Therefore the countries, especially industrialised, appropriated scientific strategies and processes, which will border the difficulties brought around via urban expansion. One of these strategies, is urban expansion administration, via using spatial suitability models in GIS, to guide expansion into areas that would lessen these difficulties to a smallest bounds. Soran city is one of the cities that attracted important curiosity of the north of Iraq, resulted in theatrical evolvement within a short retro of time.

A middle boxing a network is a device of computer networking which inspects, filters, converts or differently manipulates traffic for aims other than forwarding packet. The arrival of software defined networks means that a considerable value of current middle box functionality may has the ability to work in the centralized controller.

3. MATERIAL AND METHOD

3.1. The Research Context

The research context was in Soran-Erbil, Iraq, which is located in the northwest of Iraq, bordering Turkey and Iran as it shown in the Figure 3.1. Soran town is located about 120 km north east of Erbil, and 65 km west of the Iranian border, it also located between the high mountains of Korek in east, Goraz,hassan bag in north, Bradost in west and in south Handreen mountain, the main road of Hamilton from Erbil to Haji Omaran between 1928-1930 is extended by engineer Hamilton passing through Soran town. Today the town has a population of approximately 125000 most of which are refugees who returned from Iran to Iraq within the last ten years.

Therefore the city has been expected to continue as the population is estimated to reach 175000 in the next 10 years, the city of Soran is the field of study , it has an oval shape , it is located in a thin valley between two parallel mountains and two revers pass through the field of study one of them .

Soran town has a wet weather it has very heavy rain in winter and a hot summer, the snow level in this area is a medium in winter, a rainy spring and green ground area.

The Field of study is located between latitude 36º 37' 6" N and the longitude 44º 34' 8" E and 400 to 660 m overhead sea level.

In soran town two big rivers is passing complete it and flows to the small tributary, the Shekani river which is squirt from Iran and Balakayati region in Choman district is passing by Soran town and flows to tributary, also the Bradost river in which squirt from the high – lands of Bradost and Turkey likewise is following to the small tributary region, both rivers in the future will be useful for Bekhal bund.

Which the total area of Soran town is 4850 ha in is used for planting and agriculture, the rest of the land is inhabitancy and mountains, Soran, elevation is 660 meters.

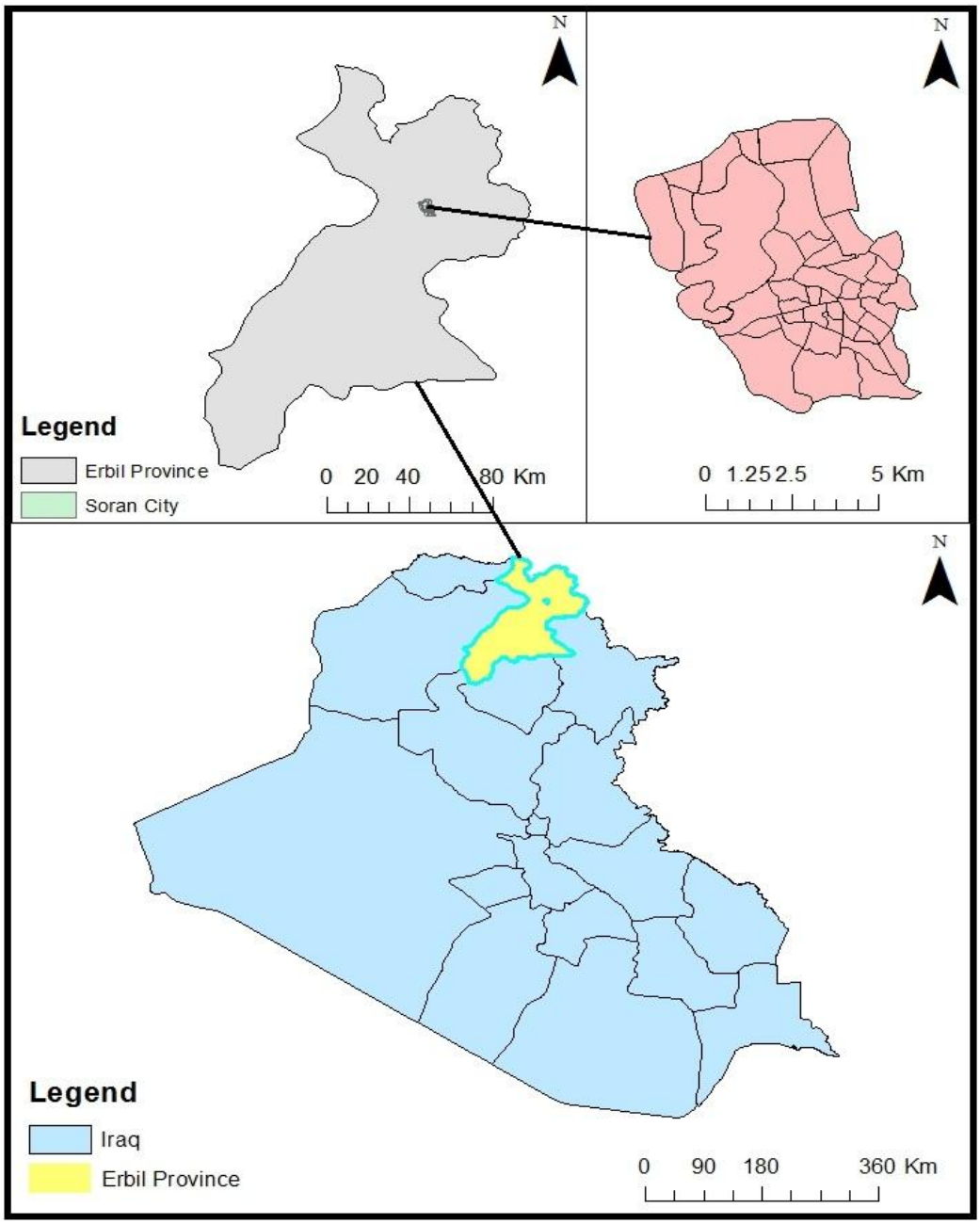

Figure 3.1. Research context

3.1.1. Geomorphological parts

In Common, Soran City falls in the little mountain zone and it's roughly 400-660m overhead sea level. Regarding the degree of sloppiness of the city is between 0-54.5 degrees. By way of it is revealed in the Figure 3.2 and landscape features of Soran City could be divided into three main parts.

3.1.1.1. Mountains

Soran is located between five mountains Korek in east, Goraz, Hassan bag in north, Bradost in west and in south Handreen mountain. The city and those mountains has taken a line shape and very few areas of these five mountains fall into the study area.

3.1.1.2. Hilly areas

This topographical region is clearly seen in the north and east areas of Soran city. Specifically, Esqala region in the east and also the areas Zaniary, Qandil, Jundian, Balakean and Bapshtian in the area. This unit is different from others because of the degree of slope 5-20 degrees.

3.1.1.3. Flat areas

Plain areas are recognized for the little degree of slope which is generally fewer than 5 degrees. And it's located in the central areas of the research place, especially in the region of Zanko, Bradost, Aelul, Galala and Handren.

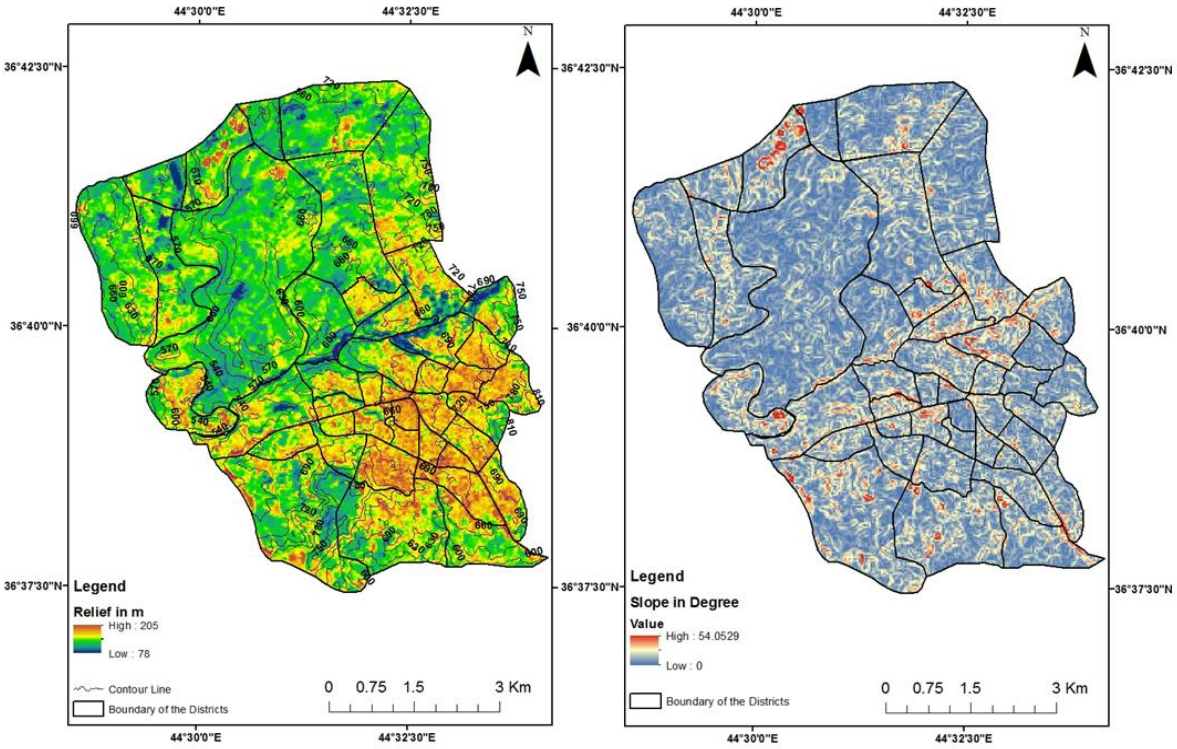

Figure 3.2. Topographic map of the study area

3.2. Data Collection

Notably, the study involved primary and secondary data to ensure that the latter complements the former while seeking to establish any parallels between the primary data collected and the existing scholarly outcomes or contributions from secondary sources of data (such as books, journals, and e-books covering the subject in related contexts). In relation to primary data collection, two Landsat images were obtained. The sources of these images were the Geo-referenced to UTM zone 38, WGS 84 and the USGS Earth Explorer website. Furthermore, the two images were sourced from Landsat-5 TM with a 16 year gap perceived to be adequate in establishing the degree of urban expansion and the resultant differences in LST within Soran-Erbil, Iraq. Explain in Tables 3.1 and 3.2.

Table 3.1. Landsat-5 TM metadata

Satellite	**landsatTM5**	**landsatTM5**
Date	16/07/1995	28/07/2011
Time	7:32:51 AM	7:27:47 AM
Image ID	LT05_L1TP_169035_19950716_20170107_01_T1_B1	LT05_L1TP_169035_20110728_20161007_01_T1
WRS Path	169	169
Row	35	35
Projection	UTM Zone 38	UTM Zone 38
Ellipsoid	WGS 84	WGS 84

Table 3.2. GIS files and secondary data used in this study

	Description
Soran map	This is in PDF file format .It describes and shows the chief land uses in the city from now until 2025.
Map of latest master plan of the city	This is in PDF file format .It describes and shows the chief land uses in the city from now until 2025.
Map of major cities in Iraq	This an ArcGIS shape file. It contains information on the Iraq Border, the main towns and governorates.

3.3. Software Used

To analyse the nature of LST variations among the images, ArcGIS 10.0 and version 9.2 of ERDAS IMAGINE 2010 were employed. Additional roles of these instruments lied in their capacity to evaluate and map the outcomes. In relation to the regression analysis and statistical analysis, Microsoft Excel was used and culminated into the presentation of data via graphs and charts.

3.4. Satellite Image Analysis

The analysis of selected images was conducted via two approaches. The first approach constituted two steps in which they were categorized by the means of supervised classification before extracting NDVI values that projected LST. The second approach involved the conversion and input of raster files into GIS environments for purposes of facilitating numerical results manipulation and the ease of calculation. Specifically, the analysis of these images entailed the adoption of the ArcGIS software to work on attribute tables. The following Figure 3.3 illustrates the steps involved in analysing the images towards better outcome provision.

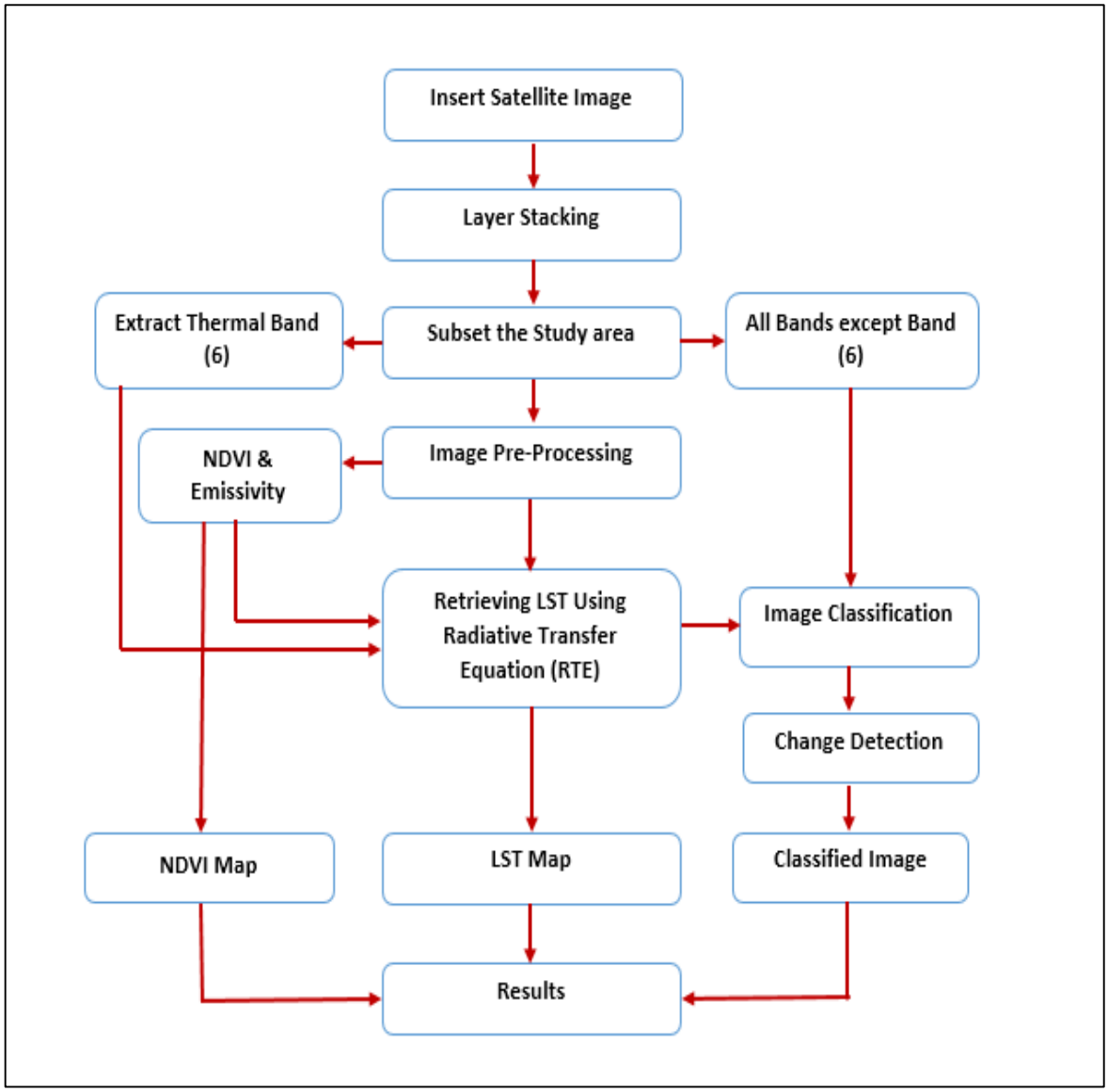

Figure 3.3. Theimage analysis process highlighted

3.4.1. The layer stacking procedure

Notably, seven different bands characterize Landsat-5 TM. Each of these bands is stored independently in Geo-TIFF file formats. Therefore, a combination of the bands to form one image leads to outcome analysis via combinations while enhancing visual-related interpretations. The following figure 3.4 show the images after performing all Landsat-5 TM bands layer stacking. Indeed, the layer stacking was performed for all bands except band 6.

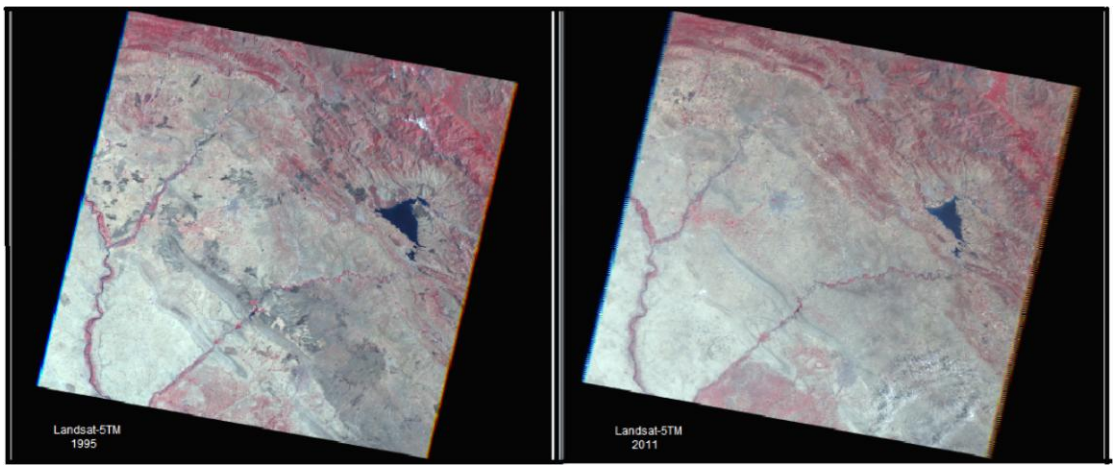

Figure 3.4. Resultant outcomes after layer stacking in relation to the Landsat images

3.4.2. Research context subset

Given the expansive nature of the initial Landsat images, ERDAS IMAGINE formed an instrument responsible for the selection of the area of interest, Soran-Erbil. Imperative to note is that the preparation of the subset area proved challenging but the aspect of remote sensing aided in simplifying the procedure. Indeed, a section of the existing literature advocates for the need to select subsets in a proper manner to ensure that it is adequately large while striving towards the provision and highlight of the target context for the specificity of the analysis (Campbell and Wynne, 2011). Then, the subset area selected is included by longitudes 36º 37' 6" N and the longitude 44º 34' 8" E as such, the total area selected was about 4850.28 hectares.

3.4.3. The pre-processing of images

The process of enhancing images aided in pre-processing. According to Lillesand et al., (2008), the primary role of enhancing images lies in its capacity to foster improvements in visual interpretability. Specifically, these improvements arise due to the better distinction of features in the target zone. Therefore, this study adopted the tasselled cap (TC) transformation to enhance the resultant images depicting the nature of the expanded urban area of Soran-Erbil. It has also been documented that TC has its operations based on albedo and brightness measuring. As observed by Armenakis et al. (2003), the extractions of these attributes arise from the responses posed by all bands in the Landsat-5 TM (except the thermal band). Studies by (Tso and Mather, 2009; Gao, 2009), revealed that the adoption of TC transformation for purposes of image analysis exhibits two main advantages. One of the

advantages is that TC transformation reduced the complexity witnessed during the classification process (through the reduction of the degree of dimensionality in the space features). Another merit is that TC transformation aids in the representation of specific concepts that characterize axes of space features in focus; including the degrees of wetness, greenness, and brightness). The representation has been documented to be achieved due to the fact that TC transformation operates on the premise of the rotation of axes; suggesting that variations among the perceived pixels. Figure 3.5. Additional documentation advocates for the adoption of TC transformation with Landsat data because it accounts for over 90 % of spectral variability available in target contexts, an observation that was made by (Armenakis et al., 2003; Healey et al., 2005; Kiage et al., 2007; Huang et al., 2010). It has been concurred further that TC transformation plays the critical role of squeezing or pressing spectral data into fewer groups that depict the actual state of physical settings (Crist and Cicone, 1984). In this study, the computation of an indicator of the TC transformation was achieved via information from six TM bands that were linked. Out of these six bands, three that are often used have been found to entail bands 1. 2 and 3.

Band 1: measures brightness in relation to the measure of differences in the degree of the reflectance of the soil while.

Band2: measures greenness in relation to the varying degrees of vegetation abundance and vigour. On the other hand.

Band 3: measures wetness in relation to the level of canopy moisture and soil interpolation.

The following Table 3.3 represents TC transformation coefficients regarding the thematic mapper for bands 1-5 and 7 regarding the functions of wetness, greenness, and brightness. Mather (2004).

Table 3.3. Represents TC transformation.

TM bands	B1	B2	B3	B4	B5	B7
Brightness	0.3037	0.2793	0.4343	0.5585	0.5082	0.1863
Greenness	-0.2848	-0.2435	-0.5436	0.7243	0.084	-0.18
Wetness	0.1505	0.1793	0.3299	0.3406	-0.7112	-0.4572

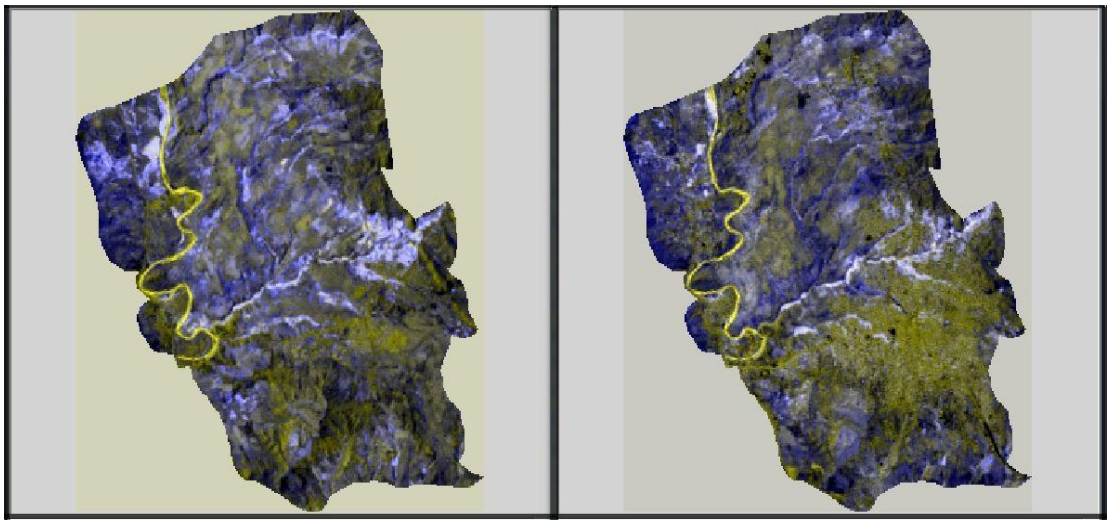

Figure 3.5. Results of TC transformation.

Urban is represented in yellow, vegetation is represented in turquoise and cadet blue, agriculture is represented in sea green and dark olive green, water is represented in yellow, and other land use is shown grey. Left image is 1995 and the right image is 2011.

3.4.4. The classification of images

In relation to the procedure of classifying images, the main aim was to assign values to digital pixels. Specifically, the values were for satellite images and reflected different classes of land cover. As observed by Mather (2004), image classification can be achieved automatically through the assignment of these pixels to form specific groups of classes that are known and are based on external data sources and analyst data while identifying each class of land. The ERDAS FILE GUIDE (2011) holds further that study objectives seeking to unearth the attribute of LST in urban zones can be achieved via the employment of monitored categorization, classifying the land cover. Five types of land cover have also been documented. The classes include water, agriculture, vegetation, urban, and other. In the following Figure 3.6. Some of the steps that were employed during the supervision of classification as adopted in this study are shown.

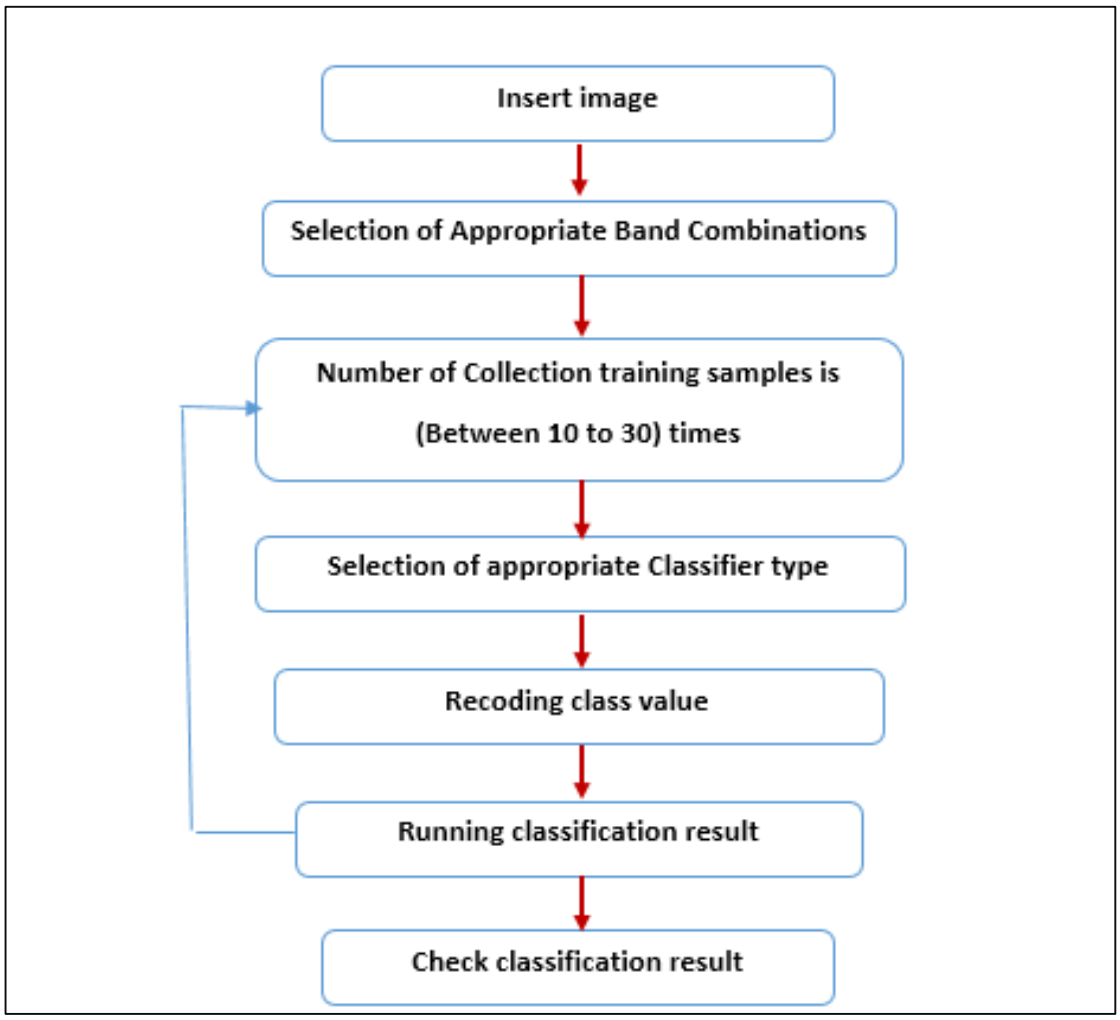

Figure 3.6. Steps followed during supervised image classification

3.4.4.1. Selecting appropriate combinations of bands

In a quest to select band combinations in an appropriate manner, this study employed the standard false colour composite. Specific bands included band 2 is green, band 4 is near-infrared and band 3 is red. Indeed, it has been asserted that the selected band combinations are highly appropriate for purposes of supervised classification in situations where Landsat-5 TM images are used (Lillesand et al., 2008; Saleh, 2011). Regarding the specific representations in relation to ground features, urban areas or man-made features are represented by grey or dark slate grey while land cover constituting vegetation is represented by shades of red. On the other hand, water is represented by dark blue while shades of green to agriculture and gold represent to other land forms. The following Figure 3.6 illustrates the respective colour representations in r elation to their depiction of landforms.

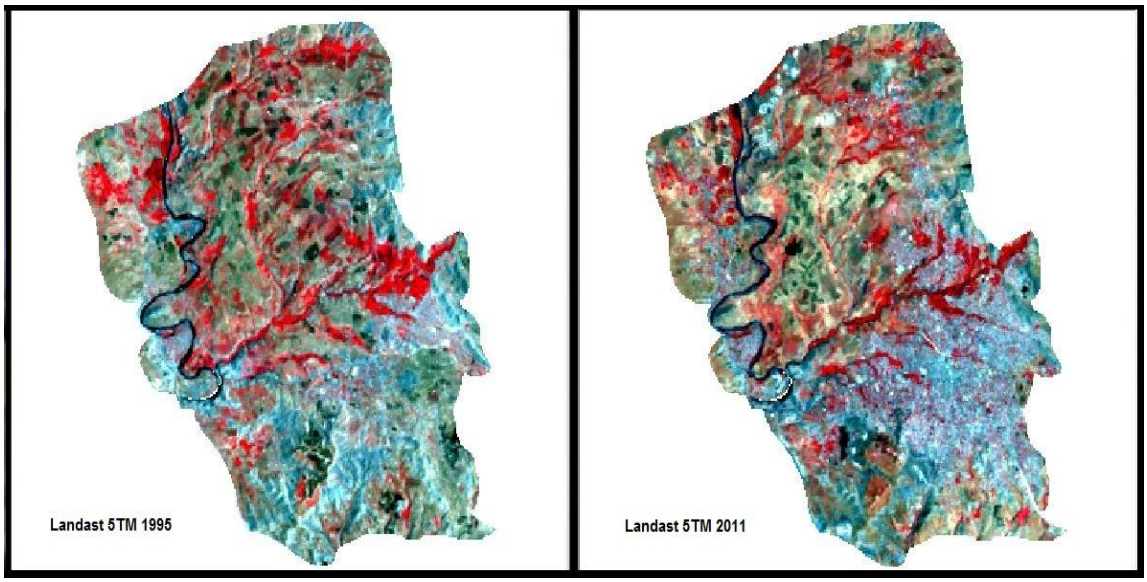

Figure 3.7. Band combinations and colour representations of landforms 4, 3 and 2 in the left for 1995 and right for 2011

3.4.4.2. The collection of training data

Informally, supervised classification has been perceived as the process through which samples perceived to have recognized identities are used. Indeed, the procedure works based on spectral pattern recognitions of the respective types of land cover in relation to pixels in satellite images (Chuvieco and Huete, 2010; Campbell and Wynne, 2011). Imperative to highlight is that selecting appropriate training samples is important because the outcomes of supervised classification are dependent on the level of expertise of the analyst. Similarly, the assembling of accurate training data is vital because it forms a predictor of success while seeking to unearth the impact of processes such as urban expansion on the degree of LST (Tso and Mather, 2009). From the recommendations by Gao (2009), four critical steps were followed during the selection process.

The first step entails the assignment of pixels into the respective classes of land cover. As noted by (Lillesand et al., 2008), an extensive distribution of land cover types over a given context requires the selection of more pixels. Specifically, 40 pixels have been suggested for the respective training samples while land cover classes have seen 20 training samples suggested. A study by Mather (2004), indicated that in situations where certain types of classifiers are likely or predicted to be common, the number of pixels in the training sample could range from 10 to 30 times the number of features housed by each class. Hence,

this study followed this first step recommended by (Gao, 2009), during the collection of training samples.

The second step entails the selection of the training sample through boundary delimitation around target pixels. Given the critical role played by the size of samples in shaping the result, an identification of the respective sizes of samples was set in such a way that it corresponded to class variations. An example of a case in which this second step is fulfilled is a case in which an area of study or research context has one water body and the sample size covers it in entirety, rather than focus on a particular section of the same.

The third step involves locating training samples. As observed by Chuvieco and Huete (2010), the role of analysts lies in the collection of samples from the entire setting to ensure that certain pixels or classes depicting specific classes of land covers are not missed. Indeed, this study followed the step to assure outcome validity and reliability.

The fourth step has been documented to involve the determination of the degree of uniformity, often depicted by spectral radiance (Gao, 2009). In this study, the fourth step was followed by ensuring that the pixels selected for the respective classes depict unimodal distributions in relation to the spectral bands utilized.

Of significance to note is that additional inputs are critical in relation to supervised classification before applying the outcomes to various algorithms. Some of the sources from which the respective inputs may be gathered include the field, maps of target contexts, reports, and air photo analyses (Mather, 2004). It has also been documented that the comprehensive understanding of geographical areas of interest and fundamental reference data need to be adopted by image analysts (Lillesand et al., 2008). The classification process has also had its success documented to lie in the aspect of ancillary data in relation to urban areas because of the latter's capacity to enhance contextual interpretations involving spatial and spectral satellite data (Chuvieco and Huete, 2010). In this study, the aforementioned aspects were achieved via maps of Soran-Erbil's master plan and Google Earth's ancillary data to collect training data.

Similarly, information from Landsat-5 TM has been perceived to constitute medium spectral resolution. As such, it becomes difficult to distinguish an urban area's forms of land cover due to the spectral characteristics; complexity as well as the presence of homogenous pixels.

Bhatta (2010), concurred that the accurate classifications of varying types of land cover that represent urban regions are difficult to achieve when Landsat imagery data is used. As such, this study's objectives were achieved by ensuring that the identification focused on the required classes only.

Specifically, the images separated by a 16 year period were classified into five categories in relation to the study's central objective. These classes included water, agriculture, vegetation, urban, and other. In relation to urban land, specific features on focus included man-made structures or infrastructure such as buildings, transportation, institutions and a residential structures. On the other hand, vegetation included grass, trees, and shrubs. In relation to the NDVI values, the vegetation was classified into the one main types in which NDVI values below 0.100 depicted a while those that would measure up to 0.100. In relation to agricultural land, this study focused on arable zones or farming activities in which regions characterized by annual replanting of crops would be considered agricultural in the land area. Water bodies were considered as those that had significant water accumulations. Thus, it was noted that some features would be man-made (Lillesand, 2008), while others would be natural. Other classes were represented by unclassified areas and the presence of barren land. According to (Anderson et al., 1976), barren land is that which is marred by limited ability towards life support and less than one third of the area is covered by vegetation; depicting an area with the dominance of rocks, sands, and thin soil.

Given that one of the leading objectives lied in the study's quest to determine the relationship between LST and the resultant nature of land cover in the urban context of Soran-Erbil, the collection of training data conformed to the aforementioned criterion. In turn, the outcomes were examined in relation to the inferences accruing from the researcher's experience in the area of study and other external sources of data. Indeed, the establishment of these classes was informed by the need to assure content- and context-specificity while seeking to understand the effect of urban expansion on the resultant state of LST, as well as the tertiary effect of LST on aspects such as land cover.

3.4.4.3. Selecting the type of classifier

According to (Gao, 2009), three main types of classifiers exist. These types include the maximum likelihood, the minimum distance, and the parallel-typed classifiers. Indeed, each of these classifiers is associated with varying merits and demerits, with the maximum likelihood and the minimum distance classifiers adopted in the majority of cases seeking to

conduct image classification. In relation to the maximum likelihood classifier, an adoption that gained adopt ion and implementation in this study, probabilities of the respective pixels belonging to the respective class sets that are predefined are calculated before assigning these pixels to classes perceived to exhibit the highest probability (Tso and Mather, 2009).

3.4.4.4. Class value re-coding

In the study, the use of the re-coding technique had its purpose lie in the need to allocate other class numbers for one or all the classes in appropriate image file formats. Therefore, the recode procedure played the critical role of input file creation via the new class numbers. Therefore, the re-coding process in this study had its aim lie in three main processes that included the need to determine new class values (using the interval, ordinal, and ratio class numbering systems), the need to integrate the classes, and the need to reduce the classes, fostering the recording process while establishing appropriate values for the respective classes. Overall, the re-coding process facilitated the process of establishing LST for the respective classes.

3.4.4.5. Classification accuracy estimation

The collection of training data sets aided in overseeing the procedure of classification. However, Tso and Mather (2009), cautioned that there is a need to ensure that the training data is adequate while excluding unrepresentative pixels. The eventuality is that the classification process is deemed complete after assessing or evaluating the degree of accuracy to determine the extent to which the analyst's level of image classification, an observation made by (Lillesand et al., 2008). Two methods have been documented to aid in accessing remote sensing images to ascertain the resultant levels of accuracy. Attributes of thematic and positional assessment have also been observed to play important roles in determining these levels of accuracy in the images obtained via remote sensing. According to Congalton and Green (2009), positional accuracy assessment implies that analysts handle information regarding the features' spatial distribution on the ground and on maps. The aim of this procedure is to establish the manner in which the features are distributed on the actual ground. On the other hand, thematic accuracy assessment implies that analysts focus on the attributes or labels of a map's features before ascertaining the possibility of the classified image labels to give true feature labels. The most commonly applied method has been observed to be the error matrix whose role lies in the selection of groups of random points

among classified images before comparing the outcomes with images representing actual scenes or feature son the ground. Therefore, accuracy assessment in this study was achieved via the collection of 326 random points for the first image 1995 and 499 points for another one 2011.

3.4.5. Change detection

According to (Singh et al., 2013), change detection plays an important role in the structure information of change thematic data because it gives an insight into the central processes related to changes in the land use and land cover. Specifically, the criticality of the change detection process fosters the comparison of LC data to the information obtained regarding the respective classes. For example, two types of tools responsible for change detection may be applied when it comes to ERDAS IMAGINE software. These tools include the matrix operation obtained via the GIS analysis menu and the change detection operation from the utilities. This study utilized the matrix operation from a GIS analysis menu towards the analysis of change detection. Specific steps included the supervision of image classification before establishing LC variations in the 1995 image and the 2011 image. In turn, a compilation was done in relation to alterations in quantitative aerial data of the respective categories' overall state of land cover or land use is exposed in Table 4.3. This reports the comparative informations, collected for each class the final map depicting changes was establishing via the labelling and clustering of the altered matrix classes.

3.5. Calculation and the retrieval of land surface temperature (LST)

From the literature review, various approaches are used to obtain LST data via remote sensing tools that focus on the thermal infrared. Despite the existence of these many techniques, three methods have been documented to be applied commonly. One of the approaches is the single-channel method that is highly applicable to sensors with one thermal band; including Landsat TM/ETM+. Another method is that which involves the split-window or two-channel approach that remains suitable for sensors perceived to have at least two thermal bands. Examples of these sensors are MODIS and ASTER. The third technique entails the temperature and emissivity separation (TES) approach, a process that was advocated by (Gillespie et al., 1998). To obtain reliable data, this study utilized the single-channel approach towards LST data retrieval. Indeed, the seclusion of the Landsat TM/ETM+ sensor was informed by the fact that it constitutes one thermal band (B6). It is

further notable that the single-channel method was adopted due to the equation transferring thermal radiance responsible for the conversion of satellite digital values into radiometric values via the high and low gain values of satellites, an attribute that was concurred by Markham and Barker (1986). The existing literature holds further that the single-channel method may assume three approaches that include Jimenez-Munoz and Sobrino (2003), algorithm, the Mono-window algorithm advocated by (Qin et al., 2001), and the Radiative Transfer Equation (RTE). This study adopted the RTE system. In relation to the atmospheric parameters obtained via MODTRAN radiative transfer, the difficulty of retrieval was handled via the use of (Barsi et al., 2005), online atmospheric correction parameter calculator. The following Figure 3.8 summarizes the process of calculating and retrieving LST, a procedure adopted by this study.

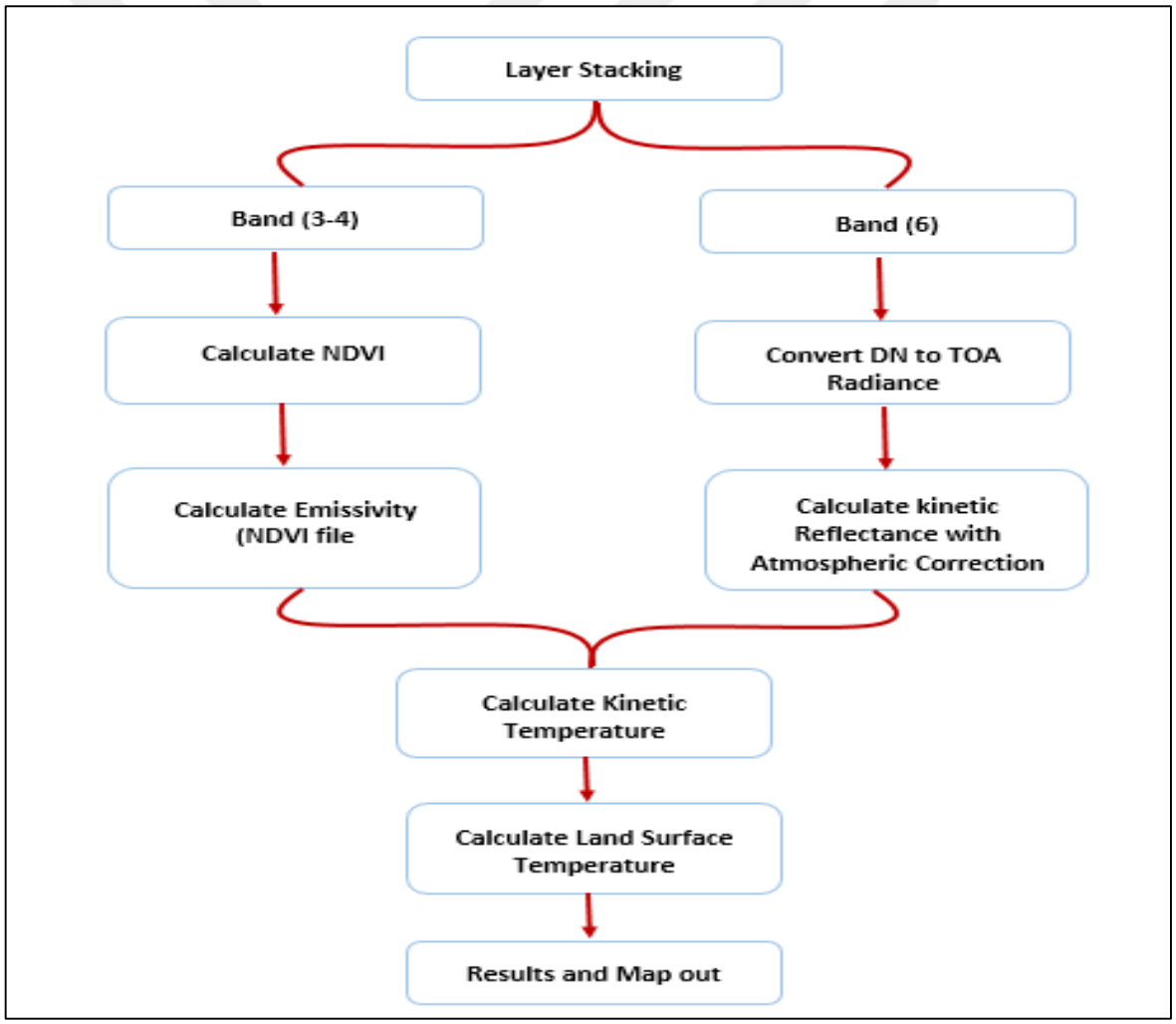

Figure 3.8. an illustration of the conversion of Landsat thermal band into LST

3.5.1. Converting digital values to radiance

The first step is converting thermal band values to radiance. The existing literature highlights that objects with temperatures above zero Kelvin are marked by electromagnetic energy emission. As such, those signals that are generated via thermal sensors of Landsat TM/ETM+ occur in the form of digital numbers (DN). And are stored in the same form. As such, the DNs were converted into the top of the atmosphere (TOA) radiance or space reaching radiance as shown in the equation that follows, (Markham and Berker, 1986; Thorne et al., 1997; Chander et al., 2002; Chander and Makham, 2003).

$$L\lambda \frac{Lmax-Lmin}{QCAL\max - QCAL\,min}(DN - QCAL\min + Lmin) \quad (3.1)$$

Where: L_λ = spectral radiance at the sensor's aperture in W/ (m^2sr μm); QCALmax = the uppermost point of the rescaled glow in DN; $QCAL_{max}$ = the lowest point of the rescaled radiance in DN (1 for LPGS, 0 for NLAPS); L_{max} = the TOA radiance that is scaled to $QCAL_{max}$ in W/ (m^2sr μm); L_{min} = the TOA radiance that is scaled to $QCAL_{min}$ in W/ (m^2sr μm).

3.5.2. Converting reflectance via the adoption of atmospheric correction

In the study, atmospheric correction played the critical role of obtaining reflectance after the conversion of the radiance values derived from computations in the first equation. As such, the process of conversion assumed the procedure advocated by Chavez (1996), who indicated that the main advantage of adopting atmospheric correction as that which aids in converting radiance values to reflectance lies in the capacity of the image itself to provide the data required for conducting atmospheric correction procedures., the atmospheric correction in relation to the earth's degree of reflectance is computed as shown in equation 2 below. (Sobrino et al., 2004).π. $(L_\lambda - L_h).d^2 \cdot ESUN_\lambda.\cos\theta_s.\tau$

$$P_p = \frac{\pi.(L\lambda - Lh).d^2}{ESUN\ \lambda.\cos\theta s.\tau} \quad (3.2)$$

In this case, τ is the degree of atmospheric transmissivity while θ_s represents the solar zenith angles, depicted in degrees. Similarly, $ESUN_\lambda$ represents the mean solar exo-atmospheric irradiance, d represents the distance from the earth to the sun and is expressed

in astronomical units, L_h is the radiance accruing from interactions between the atmospheric components such as aerosols and other molecules and the electromagnetic radiance, and ρ_P refers to the unitless planetary reflectance that is atmospherically corrected. It is further notable that equal (3.3).

$$L_h = L_m - L_1\,\% \tag{3.3}$$

(In which L_1% is one percent the dark object's theoretical radiance and Lm the radiance corresponding to the DN value of the dark object).

Lm cab be computed in Eq (3.4)

$$QCAL_{max}\quad L_m = L_{min} + DN_{min}\left(\frac{Lmax - Lmin}{QCALmax}\right) \tag{3.4}$$

Where:DNmin = the dark object DN value (minimum DN value)

The term L_1% is given by Eq. (3.5):

$$L_1\% = \frac{0.01.\cos\theta s.\tau.ESUN_\lambda}{\pi.d^2} \tag{3.5}$$

τcan be obtained according to Chavez (1996) in Eq (3.6):

$$\tau = \cos\theta_s \tag{3.6}$$

(Sobrino et al., 2004), compared Chavez's (1996) method to the simplified method for atmospheric correction (SMAC) and found that both methods resulted in similar results. For this reason, Chavez's (1996) method is rummage-sale for atmospheric correction.

3.5.3. Determining the degree of NDVI (Normalized difference vegetation index)

Spectral reflectance indices are important tools for evaluating photosynthetic traits. The normalized difference vegetation index (NDVI) is one of the maximum broadly utilized vegetation indices as an indicator of canopy green area and it is associated with grain yield as well (Tanriverdi, 2003). In studies whose central focus lies in the determination of LST, NDVI values have been found to play a leading role in shaping the nature and level of

success of the outcomes. The criticality of adopting NDVI values during the monitoring of the status of vegetation cover has also been observed to be informed by the fact that it is one of the indices that are less sensitive to alterations or variations in the atmospheric conditions (Tso and Mather, 2009). As such, this study adopted NDVI with the intention of establishing evaluations of the nature of relationship between NDVI and LST. The eventuality was a derivation of land surface emissivity, a parameter that remains vital in cases where a split window algorithm is used. The two most important Landsat-5 TM bands on focus were the red (R) band 3 and the near infrared (NIR) band 4. In this study, these two bands were adopted because green leaves or healthy vegetation has its reflectance exceeding 60 %, with the wavelengths 0.7 to 1.3μm associated with band 4. In relation to band 3, the maximum reflectance value is documented to be 20 % with the wavelengths ranging from 0.5 to 0.7μm (Gao, 2009; Tanriverdi, 2010; Zhang, 2011). Therefore, the exact NDVI values were extracted in relation to the atmospherically corrected reflectivity of Landsat TM/ETM+ bands as follows Eq.(3.7)

$$\text{NDVI}=\frac{NIR-RED}{NIR+RED}$$

$$\text{NDVI}=\frac{Pband4-Pband3}{Pband4-Pband3} \tag{3.7}$$

In this case, ρ_{band3} represented band 3's spectral reflectance while ρ_{band4} represented band 4's spectral reflectance.

3.5.4. Focusing on the ndvi and emissivity

3.5.4.1. The use of ndvi thresholds to estimate land surface emissivity

With the help of thermal infrared wavelengths, temperature estimations were achieved by measuring radiation emission by ground objects. The aim of this procedure lied in the provision of radiant temperature of target bodies because the latter shape the resultant degree of emissivity (Prakash 2000). Hence, the retrieval of data concerning the degrees of emissivity played a crucial role in achieving accurate results. Important to note is that emissivity aids in measuring the level of radiance on or in black bodies while seeking to assure the prediction of emitted radiance and its resultant level of efficiency towards thermal energy transmission into the air. Sobrino et al. (2008), asserted that emissivity (ε) ought to be known because the outcomes aid in estimating the temperature of land surfaces. In a study by Zhang et al. (2006), three methods of estimating emissivity on various land surfaces were

proposed. These forms included the use of ratio values, the use of image classification, and the adoption of NDVI values of bare ground and vegetated lands. Despite the existence of these varying forms, Ifatimehin (2007), advocated for the adoption of NDVI values due to their capacity to their ability to yield reliable outcomes regarding highly heterogeneous surfaces and vegetated surfaces. From the observation, this study adopted NDVI values while determining land surface emissivity as follows:

$\varepsilon = \varepsilon_{veg}$ if NDVI>0.5

$\varepsilon = \varepsilon_{soil}$ if NDVI<0.2

$\varepsilon = (\varepsilon_{veg}. PV) + \varepsilon_{soil}(1-P_v)$ if $0.2 \leq NDVI \leq 0.5$

In this case, $P_v$represented the fraction of vegetation cover while ε_{veg} implied the degree of vegetation emissivity. On the other hand, ε_{soil} depicted the degree of soil emissivity. As observed by Sobrino et al. (2004), the degrees of vegetation emissivity and soil emissivity can be estimated to be 0.99 and 0.99 respectively. When these values are applied and/or substituted in the equation above, outcomes may be obtained as follows:

$\varepsilon = 0.97$ if NDVI<0.2

$\varepsilon = 0.99$ if NDVI>0.5

$\varepsilon = 0.004. P_V + 0.984$ if $0.2 \leq NDVI \leq 0.5$

P_V is calculated as shown in Eq. (8) (Carlson and Ripley, 1997) similarly,

$$P_v = \left(\frac{NDVI - NDVI\,min}{NDVI\,\max - NDVI\,min}\right)^2 \quad (3.8)$$

Indeed, $NDVI_{min} = 0.2$ and $NDVI_{max} = 0.5$

3.5.4.2. Using image classification to estimate land surface emissivity

Prior to the adoption of this procedure, the role of the researcher lies in the classification of satellite images (Landsat TM/ETM+) into categories based on the nature of land cover and land use operations. For this reason, the emissivity from a pixel is determined by land objects and their emitting directions (Wan and Dozier, 1996). Some of the processing packages that can be adopted and implemented regarding this classification process include ENVI and ERDAS IMAGINE. It is further notable that the LST tool supports 10 land cover classes and land use classes on the maximum side. In turn, integer values ranging from one

to ten are assigned to the respective classes while supporting the preparation of classified images. As observed by (Watson, 1992; Snyder et al., 1998), papers that are obtained in the end can be used as sources for retrieving the emissivity values for all land cover and land use. It has been asserted further that the level of classification accuracy determines the nature of the final LST outcomes in relation to the emissivity values and classified images representing classes of land cover (Oguz, 2013). In this study, corrections targeting the effects of emissivity were achieved via the assignment of emissivity values to each category of land cover while focusing on image classification. Numerous objects have been printed guessing the emissivity standards of pulverised objects to mitigate the result of emissivity on derivative LST (Watson, 1992; Gillespie et al., 1998; Snyder et al., 1998). Snyder et al., (1998), situations that correction of the result of emissivity can be attained by transfer an emissivity price to apiece land cover category of the classification image. According to the literature land surface emissivity varieties from 0.950 to 0.990 (Lillesand et al., 1994; Nichol, 1994; Snyder et al., 1998).

3.5.5. Kinetic temperature calculation

Given that this was an absolute temperature study, it was important to remove atmospheric effects. Barsi et al. (2005), affirmed that the atmosphere tends to attenuate the ground's energy emission. To address these potential impacts of the atmosphere, TOA or space-reaching radiances were converted to achieve surface-leaving radiance. Specifically, the MODTRAN radiative transfer (an atmospheric correction tool) was applied. Some of the parameters that the tool aided in estimating included the down-welling radiance, the upwelling radiance, and the atmospheric transmission. Upon retrieving these parameters, TOA or space-reaching radiances were determined and converted into surface-leaving radiances. The following equation illustrates the conversion process adopted by this study while striving towards the realization of surface-leaving radiances with the Eq. (9) (Barsi et al., 2005).

$$T_T = \frac{L\lambda - L\mu - \tau\,(1 - \varepsilon)Ld}{\tau.\varepsilon} \tag{3.9}$$

Indeed, black body targets, which had kinetic temperature (T), were depicted by radiance (L_T). On the other hand, L_λ constituted the top of atmosphere or space-reaching radiance while L_μ formed the atmospheric of upwelling path radiance. Similarly, ε formed

the surface's emissivity, τ the level of atmospheric transmission, and L_d the sky radiance or down-welling.

3.5.6. Calculating land surface temperature (LST)

From Planck's function, the achievement of satellite brightness temperature upon converting spectral radiance lies in the alteration of DVs into the spectral radiance. Whereas the current study adopted an alternative equation, the outcomes were similar to those that would have been obtained in a situation where Planck's function was used. The specific equation adopted was that which was advocated by Markham and Barker (1986), which holds that a unit radiance comes in the form of W/ (m^2srμm) while the aspects of emissivity and transmission remain unitless. To determine the degree of land surface temperature, the following equation was adopted:

$$T = \left(\frac{\mathrm{K2}}{\mathrm{in}\left(\frac{k1}{LT}\right)+1} \right) \text{-}273.15 \qquad (3.10)$$

Specifically, T represented the level of brightness temperature of the satellite in Celsius while K_2 and K_1 indicated Landsat TM's spectral radiances in Band 6 at 1260.56 and 607.76 respectively. On the other hand, L_T constituted the spectral radiance of the satellite.

3.6. Outcome conversion into GIS contexts

According to Hodgson and Jensen (2005), data that has been obtained via images that are remotely sensed tends to occur in terms of pixel values. The pixels are representations of ground locations via X, Y information. Indeed, the outcome is responsible for the remote derivation of information that is applied in relation to other information in the modelling procedures that include GIS. By converting data that is remote sensed into GIS settings, geographical and numerical analyses are achieved. A specific example of this application is a case in which LST's mean values are extracted for the respective districts and classes of land cover to map out the outcomes accordingly.

In this study, the perceived or intended objectives were achieved via the use of the GIS approach during the analysis and evaluation of spatial data. For example, all the outcomes were directed to the ArcGIS software that aided in the reclassification of raster images, upon which raster-grids were obtained. Indeed, image reclassification played the

crucial role of value moderation in the given inputs while achieving alterations or changes to the output raster that resulted. The eventuality was the production of unique values, with the class freed of the background. In turn, the reclassified images were combined with LST image outcomes for the respective classes. This conversion of the results into a GIS environment culminated into the conversion of the town's city maps into a polygon shape with the aim of achieving independent LST values representative of each district. The following Figure 3.9 illustrates the summary of the methodology used during the data collection process, a process that formed a foundation for obtaining the findings, providing the discussion, inference making, and the conclusion and recommendations regarding the impact of urban expansion on attributes such as LST.

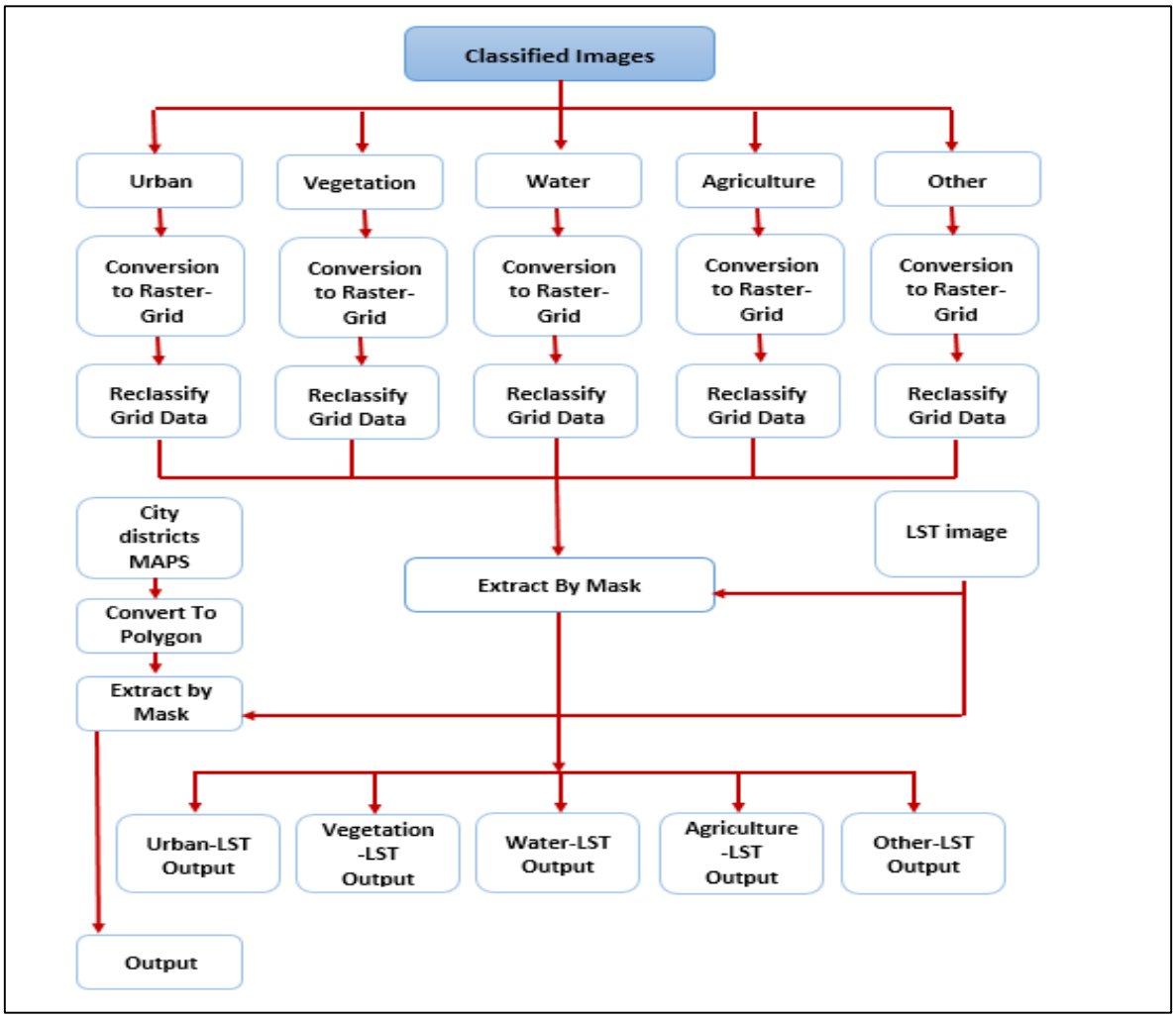

Figure 3.9. An illustration of the outcome conversion into vector file formats (from raster file formats) in GIS contexts

4. RESULTS AND DISCUSSIONS

4.1. Outcome classification

To achieve the process of land cover class categorization in relation to the accompanying detection of alterations in the various categories of land cover classes between the years 1995 and 2011, this study utilized the supervised classification approach. As it show in the Figure 4.2 and 4.3. Notably, the utilization of the supervised classification procedure was based on Landsat-5 TM. From the findings, the 16 year period is marked by significant variations in the nature of land cover. Specifically, the grey colour on images depicted urban land containing roads and buildings while the red colour represented vegetation in the entirety. On the other hand, while the rest of the features saw the blue colour represented water accumulation and agricultural land depicted by the green colour. Gold colour represents the latter aided further in depicting land surfaces with rocks, sand, and thin soil.

Specific outcomes indicated that the target region had the 1995 image depicting the presence of vegetation and accounted for about 17.46 % of the entire land. Later, the image depicting the physical nature of the landscape saw the area under vegetation reduce significantly to just over 11.8 % of the land cover. Hence, the urban land in Soran-Erbil was noted to have undergone significant alterations or changes in terms of the physical environment or landscape. Large-scale and fast expansions are observed to have accounted for these significant changes in the target zone. One of the effects of this reduction in the degree of vegetation in Soran-Erbil area remains attributed to the issue of climate change whose trickle-down effect is felt in terms of drought. Another reason accounting for the reduction in the cover of vegetation is seen to lie in the decline in water levels of capacities. A reduction in agricultural land cover (as a consequence of urban expansion) is also seen to assume a related trend whereby the cover was about 13.44 % in 1995 but urban-related activities have seen the decline read about 11.4 % of the cover; attributed to built-up areas in relation to urban activities that are ever expanding in Soran-Erbil, Iraq. In relation to water and other classes of land cover, an increase in coverage is observed. With the increase indicating a 1995 reading of 4.34 % to 2011's 1.37 %, the trend is attributed to the higher presence of man-made dams perceived to collect water during rain seasons, with the two images collected in close months. Therefore, changes in water cover were less significant when compared to other features while other classes revealed an increase from 19.76 % 1995

to 18.14 % 2011. In summary, the 16 year period revealed a 12.26 % increase in urban land coverage due to the process of expansion. Regarding specific classes, vegetation decreased by 5.66 %. Similarly, land cover under agriculture and because of urban expansion in Soran-Erbil was found to be 2.04 %. Water bodies or coverage decreased by a less significant percentage at 2.97 % while other features revealed a decrease in cover of 1.62 %, see Table 4.1.

The following Figure 4.1 illustrates a summary of this study's outcomes regarding the nature of urban expansion and its resultant impact on the various classes of land cover.

Table 4.1. Summary results of LU/LC change between 1995 and 2011

Class name	Area in(ha) 1995	Area in(ha) 2011	Coverage 1995%	Coverage 2011%	Changes %	Remark
Urban	2181.51	2777.67	44.97	57.26	12.26	**Increase**
Vegetation	847.17	572.76	17.46	11.8	5.66	**Decrease**
water	210.78	66.87	4.34	1.37	2.97	**Decrease**
Agriculture	652.14	553.05	13.44	11.4	2.04	**Decrease**
Other	958.68	879.93	19.76	18.14	1.62	**Decrease**
Sum	4850.28	4850.28	99.97	99.97	24.55	

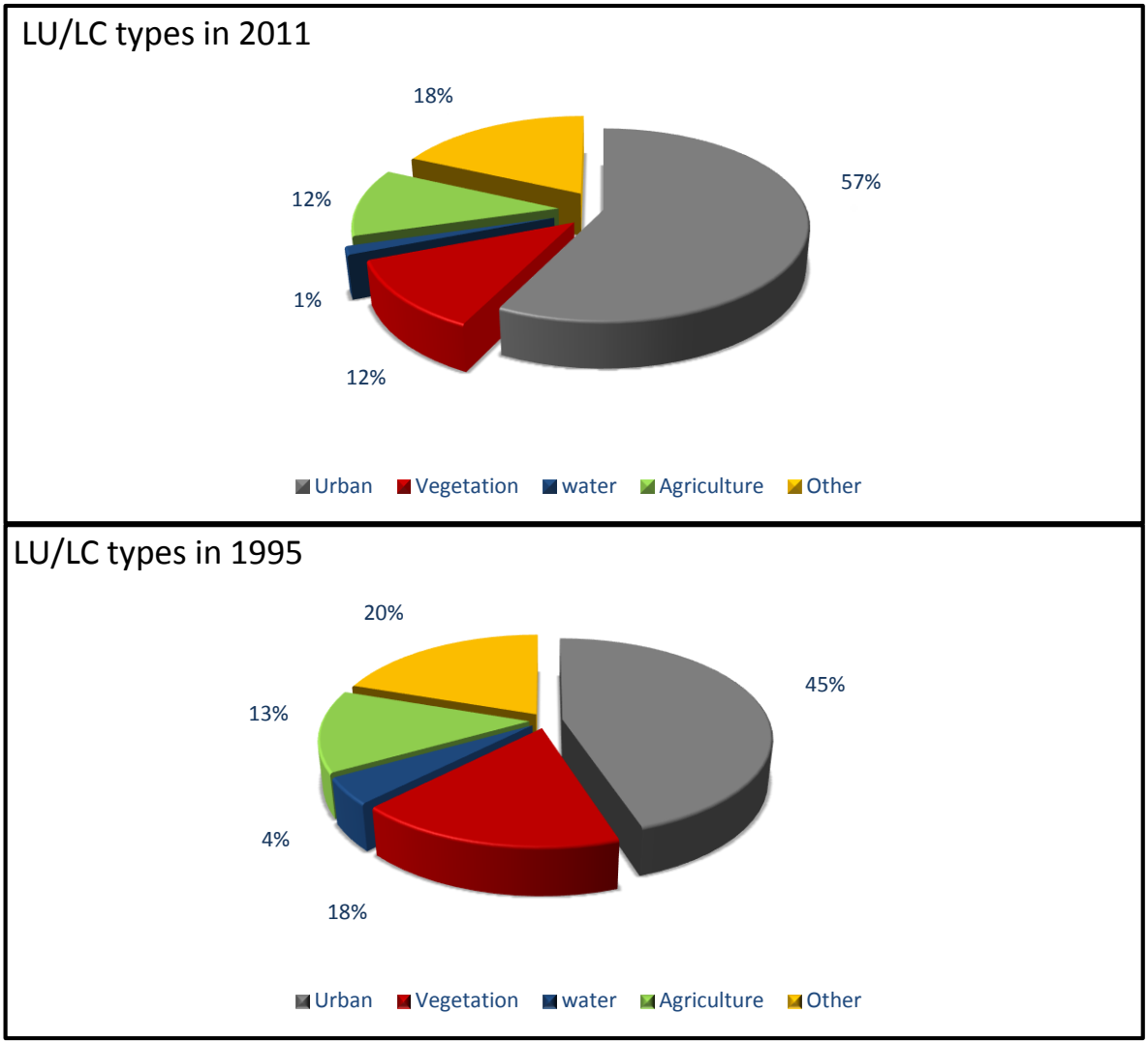

Figure 4.1. Changes in land cover due to urban expansion in Soran-Erbil

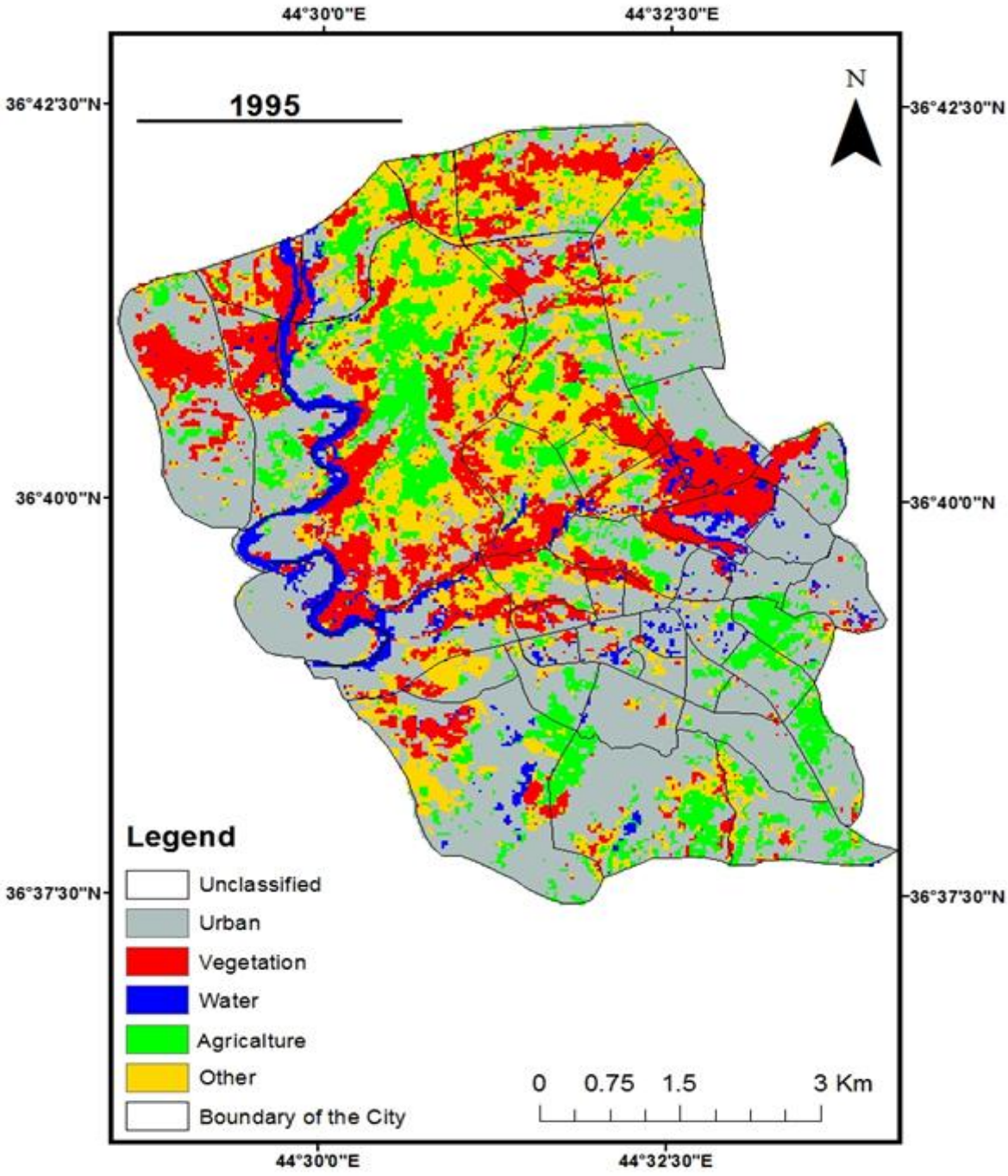

Figure 4.2. Changes in land cover as observed in the 1995 image

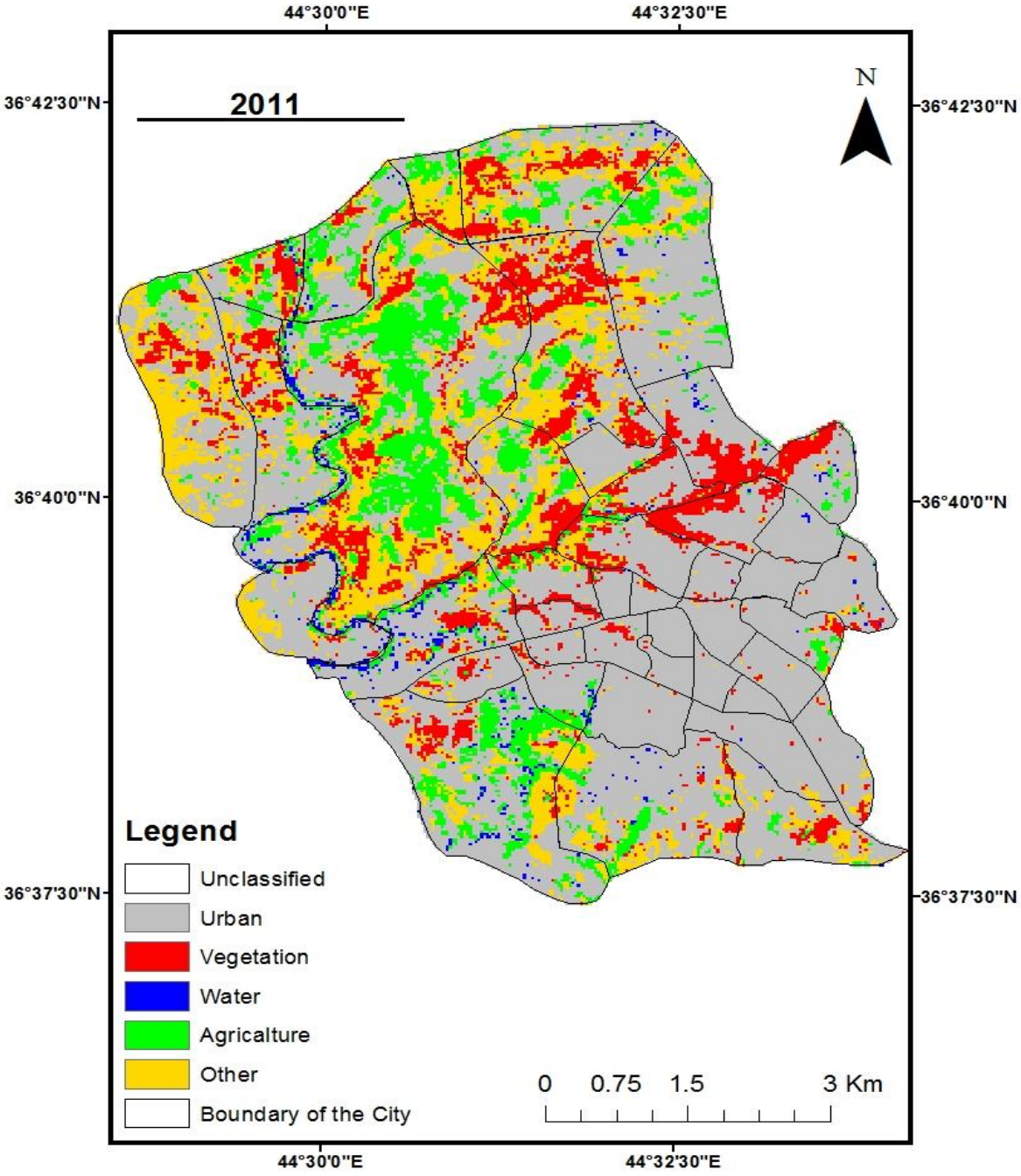

Figure 4.3. Changes in land cover as observed in the 2011 image

4.1.1. Focusing on the assessment of accuracy

After the process of classifying the land cover, this study proceeded to assess the degree of accuracy in relation to the resultant classification of various classes or categories of land cover. Notably, the study employed the error matrix approach. Specifically, a total of 326 points were selected randomly for purposes of assessing the degree of accuracy of the classification process for 1995 image and 499 points for 2011 image as shown in Figure 4.3.

With a kappa 0.93, the degree of accuracy of the image representing the land cover of Soran-Erbil in 2011 was 96 %. On the other hand, the 1995 image had a kappa 0.93 and had its degree of accuracy in relation to the classification process lie at 95 %. From the findings, it can be inferred that the findings were highly reliable and valid because of the significant level of assessment accuracy achieved. These outcomes are depicted in the Table 4.2.

Table 4.2. Classification accuracy for years 1995 and 2011

The result of error matrix in 2011

	Urban	Vegetation	Water	Agriculture	Other	Line total	Producer's Accuracy %	User's Accuracy %
Urban	299	3	3	2	1	**308**	99.01	97.08
Vegetation	1	53	1	0	1	**56**	92.98	94.64
water	0	0	4	0	0	**4**	44.44	100
Agriculture	1	0	1	57	0	**59**	93.44	96.61
Other	1	1	0	2	68	**72**	97.14	94.44
Top raw	**308**	**56**	**4**	**59**	**72**	**499**		
Classification Accuracy = 96.39%								
Kappa Statistics = 0.9377								

The result of error matrix in 1995

	Urban	Vegetation	Water	Agriculture	Other	Line total	Producer's Accuracy %	User's Accuracy %
Urban	134	4	2	1	2	**143**	97.84	93.79
Vegetation	2	55	0	0	0	**57**	88.71	96.49
water	0	1	13	0	0	**14**	86.67	92.86
Agriculture	1	0	0	43	0	**44**	95.56	97.73
Other	0	2	0	1	63	**66**	96.92	95.45
Top raw	**145**	**57**	**14**	**44**	**66**	**326**		
Classification Accuracy = 95.09%								
Kappa Statistics = 0.9315								

4.2. Analysing change detection

4.2.1. Focusing on the 1995-2011 period

In re mote sensing practices, change detection aids in determining potential alterations or variations in the nature of features over a given period. For example, change

detection aids in highlighting spatial characteristics and quantitative and qualitative data outcomes in relation to changes in the land cover features. Specific attributes on focus in this study included an examination of the type of changes experienced such as boundary variations and ground type or surface changes. In relation to the 1995 and 2011 images, this study established that there was a significant increase in urban expansion in Soran-Erbil while some of the classes that included agricultural land cover and vegetation witnessed a significant decline in coverage. Indeed, it was inferred that the change in the nature of land cover in this research context was due to the people's movement or migration to urban regions, a spatial trend characterizing the period ranging from 1995 to 2011. With the grey colour depicting change. As shown in Table 4.3, the outcomes of change detection and its accompanying analysis are presented in the following Figure 4.4.

Table 4.3. Change detection between1995-2011.

	1995 LULC (ha)					
2011 LULC (ha)	**Urban**	**Wegetation**	**Water**	**Agriculture**	**Other**	**Class total**
Urban	17406.00	2239.20	952.20	3241.80	3937.50	27776.70
Vegetation	674.10	3463.20	185.40	293.40	1111.50	5727.60
water	289.80	19.80	319.50	16.20	23.40	668.70
Agriculture	1104.30	285.30	542.70	2004.30	1593.90	5530.50
Other	2340.90	2464.20	108.00	965.70	2920.50	8799.30
Class Total	21815.10	8471.70	2107.80	6521.40	9586.80	.....
Class Change	4409.10	5008.50	1788.30	4517.10	6666.30	.....
Image difference	5961.60	-2744.10	-1439.10	-990.90	-787.50	.....

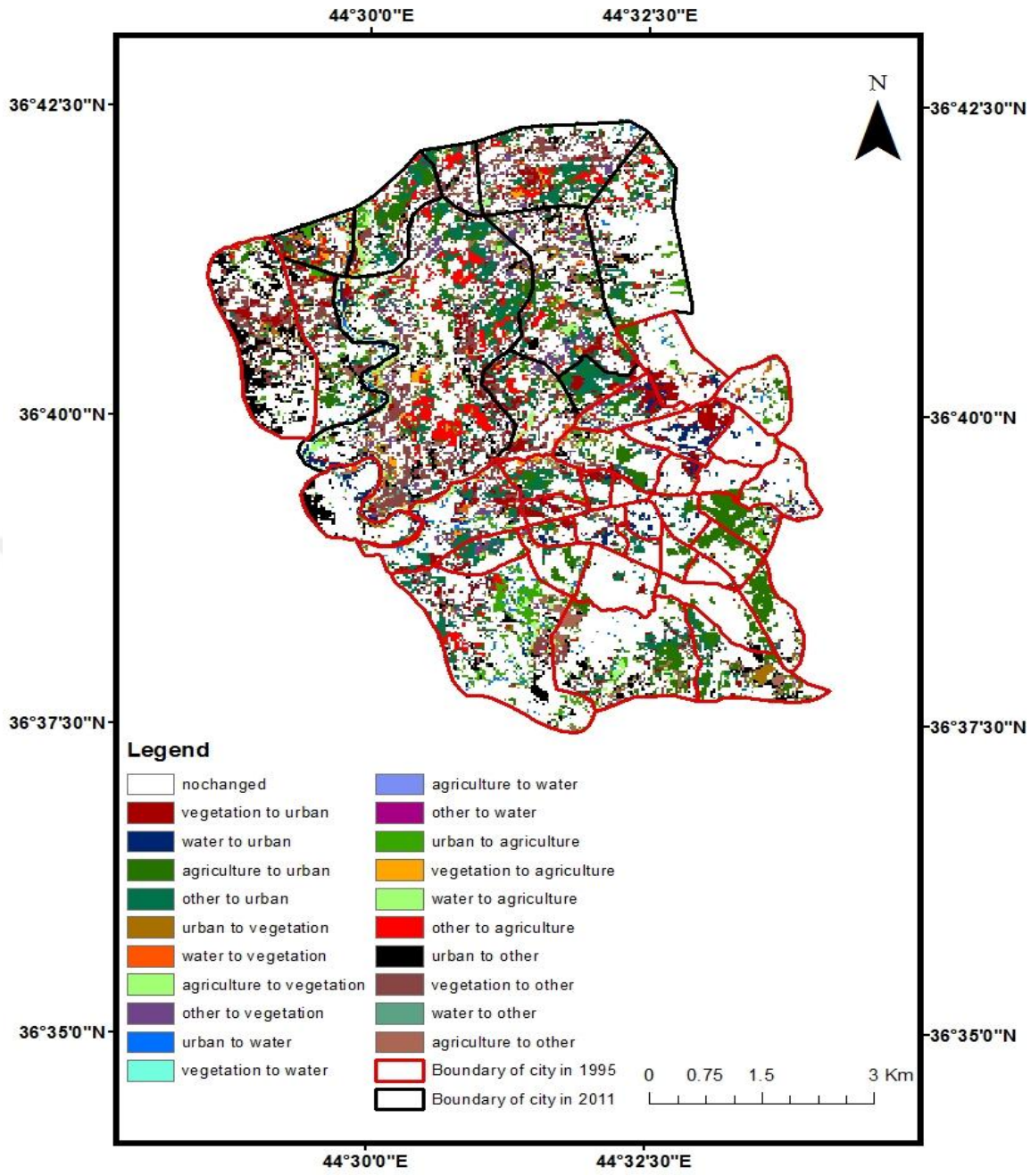

Figure 4.4. Change detection between the years 1995 and 2011

4.3. Land surface temperature retrieval

As mentioned earlier, this study adopted the Radiative Transfer Equation (RTE) during the retrieval of land surface temperature for Soran-Erbil. The aim of the RTE equation was to promote the mapping out of LST spatial variations between the years 1995 and 2011. It is further notable that the RTE equation was used alongside the GIS method for purposes

of allowing geographical and numerical analyses of LST temporal and spatial distribution. Upon mapping out the resultant states of LST temporal variations during the 16 year period, sequential colours representing various degrees were obtained and highlighted as shown in the Figure below 4.5.

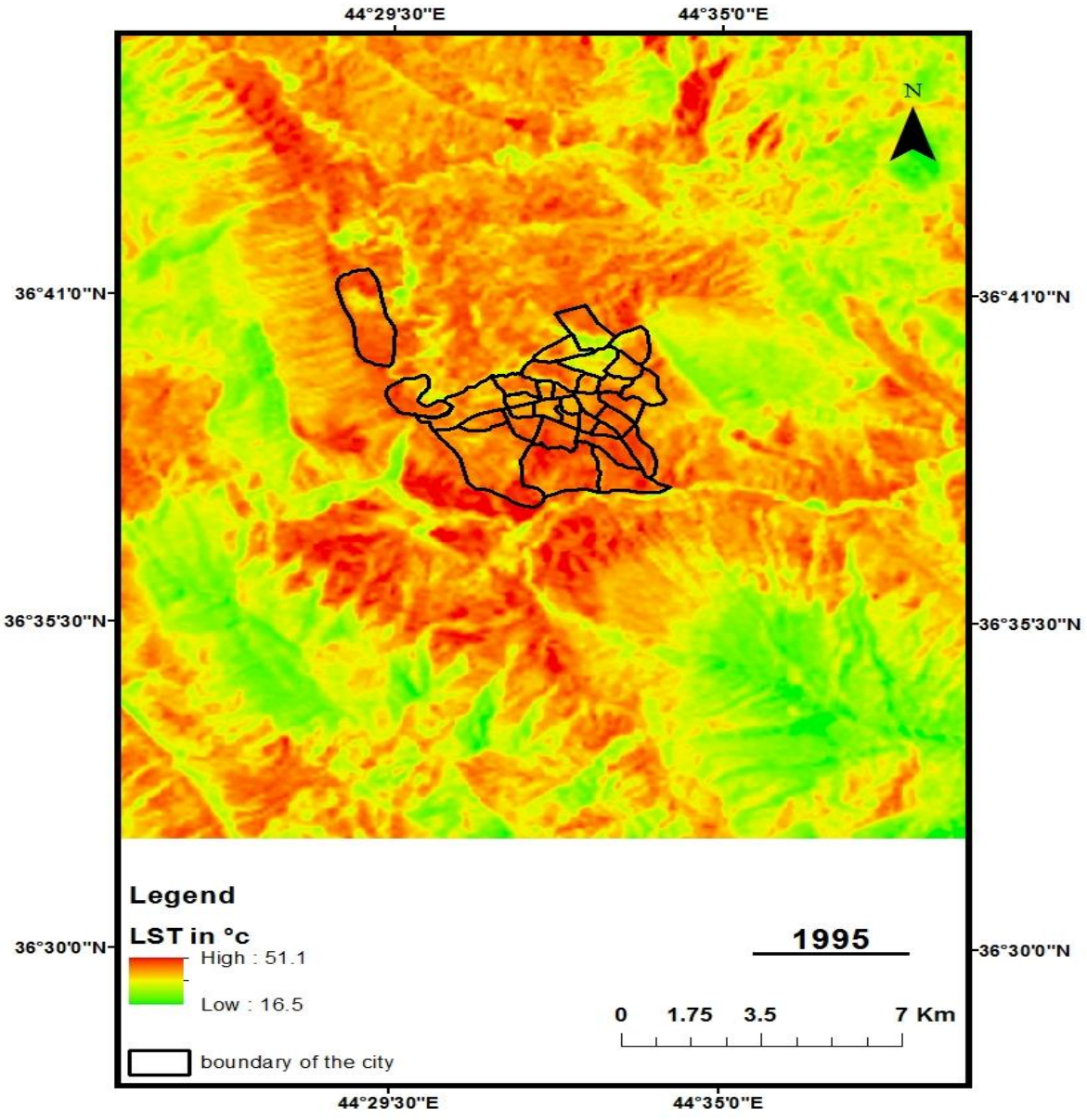

Figure 4.5. LST outcomes for the year 1995

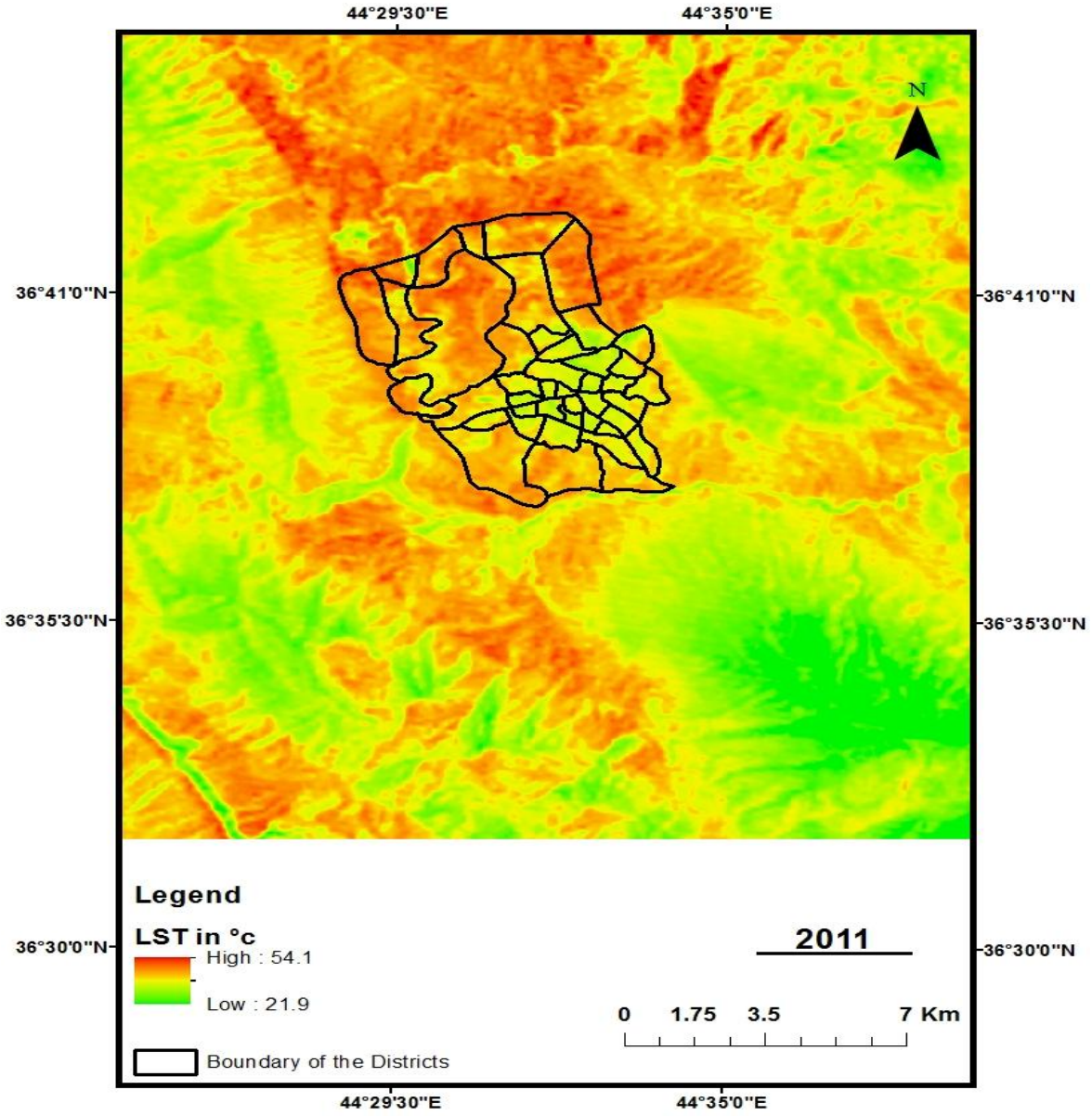

Figure 4.6. LST outcomes for the year 2011

The LST results shown in Figure 4.6 from deferent years above, the two images indicate that the hottest regions lie outside the urban zone of Soran-Erbil. On the other hand, cooler regions are seen to lie within the urban region as well as water bodies or accumulations and other classes of vegetation. As such, the LST outcomes obtained by this study failed to concur with a majority of the existing literature, which highlights that urban areas exhibit a higher likelihood of experiencing higher temperature when compared to the surrounding or neighbouring zones. The inference is informed by the findings in which the LST values within the urban zone are lower than the values obtained for regions outside the

city in both years. However, the outcomes concur with the findings by (Kwarteng and Small, 2005; Ahmed et al., 2005; Habib, 2007; Bounoua et al., 2009). Regarding the change in temperature, the study established an LST increase by five degrees Celsius when the total area was examined and the maximum LST increased by 3 ºC, reaching 51 ºC in the year 2011 when compared to 1995's value of 54 ºC. Similarly, the least LST value was found to increase 6 ºC from 16 ºC for the year 1995 to 22º C for the year 2011. Various factors were also found to be attributable for the resultant changes in the minimum and maximum LST at Soran-Erbil. One of the factors included time variations regarding when the images were taken. Another reason entails significant environmental problems that the region may have faced in the 16 year period. These effects include drought and desertification. The third factor involves a significant decline in vegetation cover, an aspect that this study found to pose a direct influence on the resultant state of LST value. Specifically, groups of vegetation such as agricultural, and vegetation revealed a decline from 55 % to 42.71 % in the 16 years period. The trickle-down effect of this reduction was attributed to the decline in the level of humidity. Notably, the significant increase in the maximum LST (that depicted a range of five) was linked to potential errors in the approach associated with pixels, with satellite image-retrieved LST temperature dependent on the degree of reflectance of the pixel. As such, a higher pixel reflectance is likely to have led to higher LST; attributed to operations such as construction activities at the time the image was taken in 2011.

4.4. Land surface temperature spatial distribution

According to Voogt and Oke (2003), LST retrieval in an urban zone is highly dependent on the nature of balance of the surface energy. Therefore, differences in LST distribution in an urban zone remain dependent on the nature of building construction materials that include mud, rock, concrete, and asphalt. In addition, LST distribution is shaped by differences in the type of land cover, including water, green regions, and buildings. In this study, GIS approaches were employed towards the investigation of LST spatial distribution and this step aided in the identification of the region's cool and hot zones.

Image data in 1995, the spatial LST patter was non-concentric and non-equal Figure 4.6 and 4.7 and Table 4.4. Therefore, the highest temperatures were associated with regions located close to the urban region of Soran-Erbil. For example, Sarchan, Balakian, Xabat, Bapshtian, Bnar, Goraz, Nahri , Barxudan, Zozik, Raparin, Isqalla, Jundian were identified as having the hottest surface temperatures 43, 42, 42, 42,41, 41, 40, 40, 40, 40, 40 and 40

ºC, respectively. The cause of this trend was that which lied in the presence of hard surfaces or open areas in these regions located around the urban zone, having little or no cover. In addition, it is important to note that other hot place was found in the district of Sarchan. The presence of buildings with aluminium roofs formed another factor responsible for the high temperatures around the urban zone. Specifically, these roofs would emit thermal energy because of activities in institutions such as factories. Furthermore, the districts which were newly built during this period have a higher surface temperature compared with older zones. For instance, Shahidani Delzian and Zanko, which were new districts built in 2011, have an LST of 44 ºC and 45 ºC.

Regarding the 2011 data, dissimilar outcomes were received in such a way that the spatial LST patter was neither concentric nor equal. However, urban expansion accounted for the changes in LST when compared to the 1995 data because of a lake of vegetation cover (Gartland, 2008). Therefore, the mean LST for the former year was higher when compared to the latter year (as revealed by this study). The newly built districts in both years exhibited different outcomes in terms of recording higher temperatures when compared to the LST data revealed by older districts. The outcomes discovered that the expansion of the city over the dry lands surrounding the city led to a decrease in LST of about 2°C in some anew built districts as can be seen from the blue colour on the map, though the red colour mentions to an increase in LST of more than 2°C thus, the expansion of Soran City over the other land cover in this region has led to a control and discount of LST see Figure 4.9.
This outcomes completely matches that of other studies which were 47 done in near like geographical situations such as the studies by Habib (2007), Kwarteng and Small (2005), Frey et al. (2005), in which they pointed out that constructing buildings over dry and desert land is a way to control the increase in LST and produce urban cool islands (UCI).

Table 4.4. Give the following data: Mean LST in ºC of main districts in Soran City on 16-07-1995 and Mean LST in ºC of main districts in Soran City on 28-07-2011.

No	name of districts	mean LST in ºC 1995	mean LST in ºC 2011	NO	name of districts	mean LST in ºC 1995	mean LST in ºC 2011
1	Sarchan	43	43	**23**	Dilman	39	40
2	Bnar	41	45	**24**	Zaniyary	38	40
3	Kani	39	41	**25**	Bapshtian	42	43
4	Balakian	42	42	**26**	Isqalla	40	43
5	Goraz	41	42	**27**	Wasta Rajab	39	41
6	Brayati	36	39	**28**	Jundian	40	42
7	Diyanaykon	34	38	**29**	Sarwaran	39	40
8	Srwa	38	39	**30**	Azadi	37	40
9	Baxtiyari	38	38	**31**	Sarwuchawa	39	39
10	Aylul	37	38	**32**	Korek	39	42
11	Nawroz	38	39	**33**	Barzan	40	41
12	Galala	39	40	**34**	Qandil	40	42
13	26 Gulan	38	38	**35**	ZawiBatal	38	40
14	ChamiRezan	38	39	**36**	ShahidaniDelzian	-	44
15	Nahri	40	42	**37**	ZawiBatal	-	43
16	Barxudan	40	40	**38**	Bradost	-	42
17	Zozik	40	42	**39**	Xwakurk	-	42
18	Raparin	40	41	**40**	Awara	-	42
19	Handren	39	40	**41**	Zanko	-	45
20	Harem	39	40	**42**	Cham	-	45
21	Xabat	42	39				
22	Shorsh	37	39				

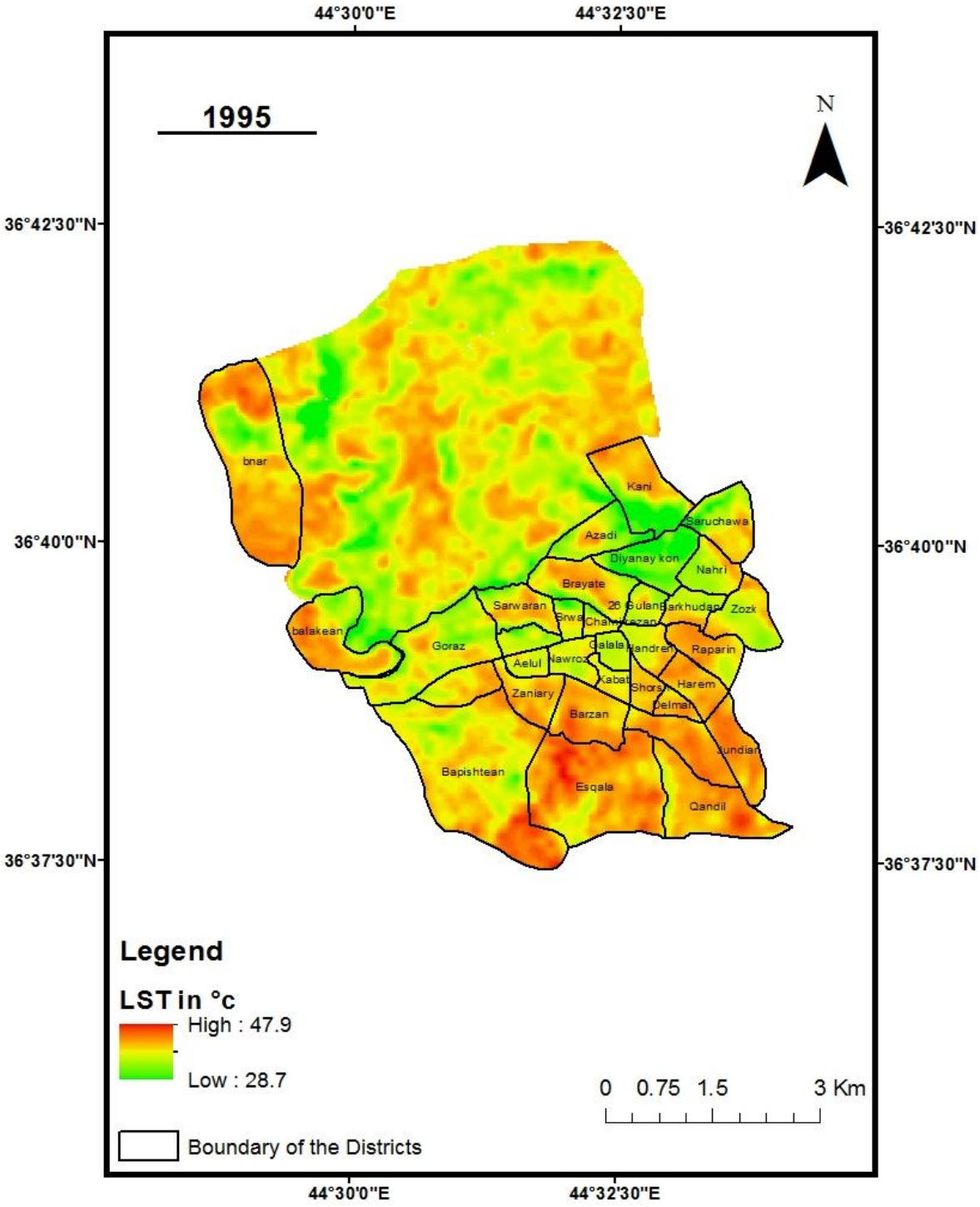

Figure 4.7. Spatial distribution of LST in the main districts of Soran City on 16-07-1995

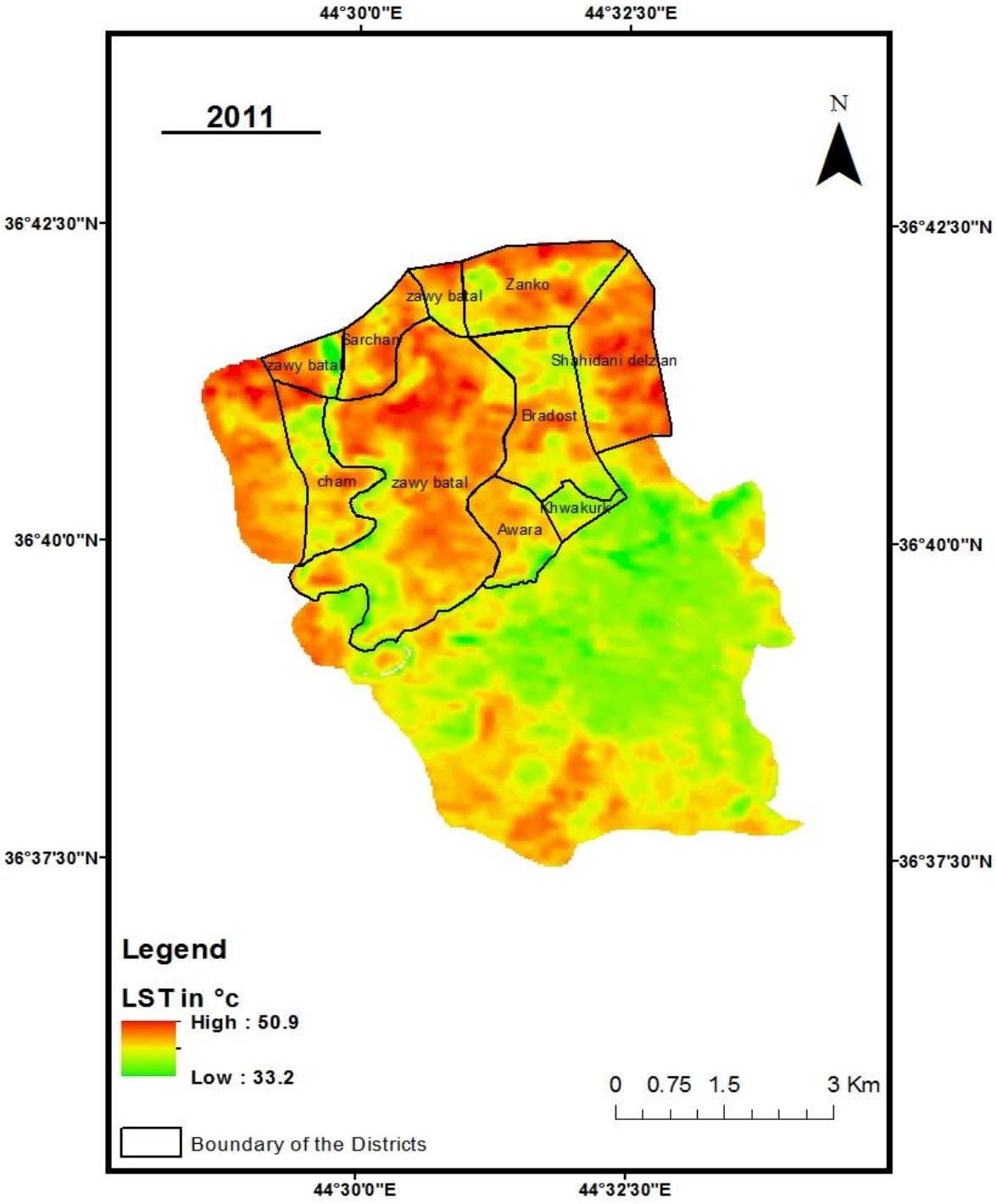

Figure 4.8. Spatial distribution of LST in the main districts of Soran City on28-07-2011

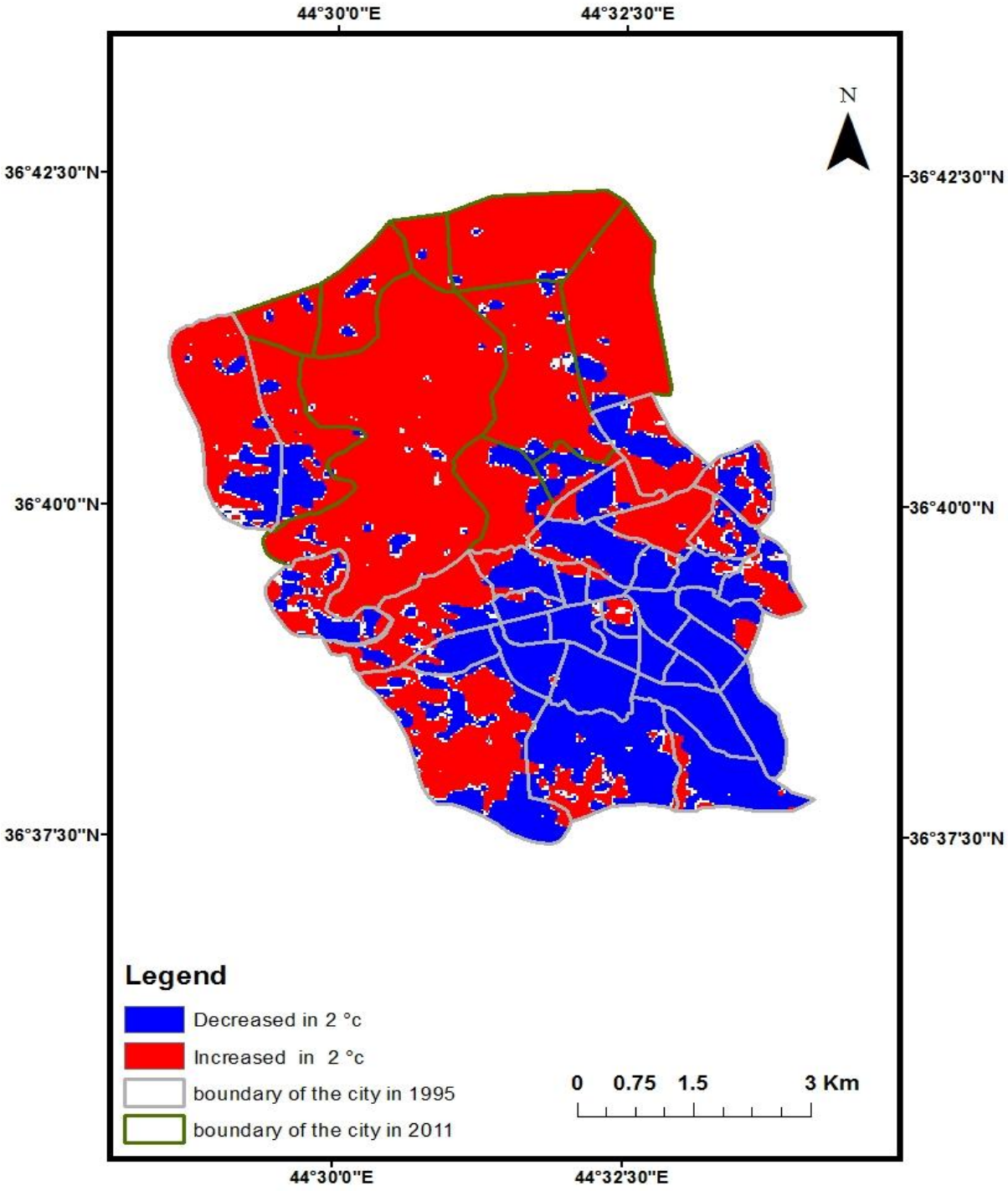

Figure 4.9. Change detection map based on LST for 1995 and 2011

4.5. Examining the correlation between LST and various land covers and land uses

From the findings, differences in LST are dependent on a number of factors that affect the ground's heat processing; including vegetation abundance, albedo, emissivity of the land surface, and the level of soil moisture (Weng et al., 2004). Hence, each form of land cover is unique and plays a similarly unique role in shaping the nature of LST. In a quest to establish the relationship between LST and various land covers, LST maps and the classified images were exported to the ArcGIS software to link the respective classes with LST values. The eventuality was the extraction of the mean LST for the respective types of land cover. With alterations in environmental and climatic conditions of the region, a general increase in LST was observed when the overall outcomes obtained from the 1995 image were compared to those of 2011. Specific, areas with vegetation were marked by a temperature of 34 ºC in 1995 when compared to 40 °C for the year 2011 in Soran-Erbil. Similarly, water bodies recorded the lowest temperature in the 16 year period in which the study established 33 °C for the year 1995 while the outcomes for the year 2011 revealed 38 °C. Despite the presence of the least temperatures for both years in relation to regions with water bodies or water accumulation, it was still evident that an increase in temperature was evident and the outcome concurred with the findings established regarding other land covers such and vegetation. Hence, in recorded cases, the 'other class' consisted of barren land which typically records a high LST due to the lack of vegetation to save the land from the warmth of the sun, and any transpiration cooling due to the existence of plant life (Weng et al., 2004).

Notably, the highest LST value was established for other land covers and open classes when compared to the urban land cover due to the potential impact of the time when these Landsat TM images were taken. Specifically, the images had been taken during the mid-morning hours and, as observed by Abdullah (2012), urban areas are more likely to become warmer on a slower basis and cool more slowly. The following Figure 4.10 illustrates the mean LST values for the various land cover classes in the years 1995 and 2011.

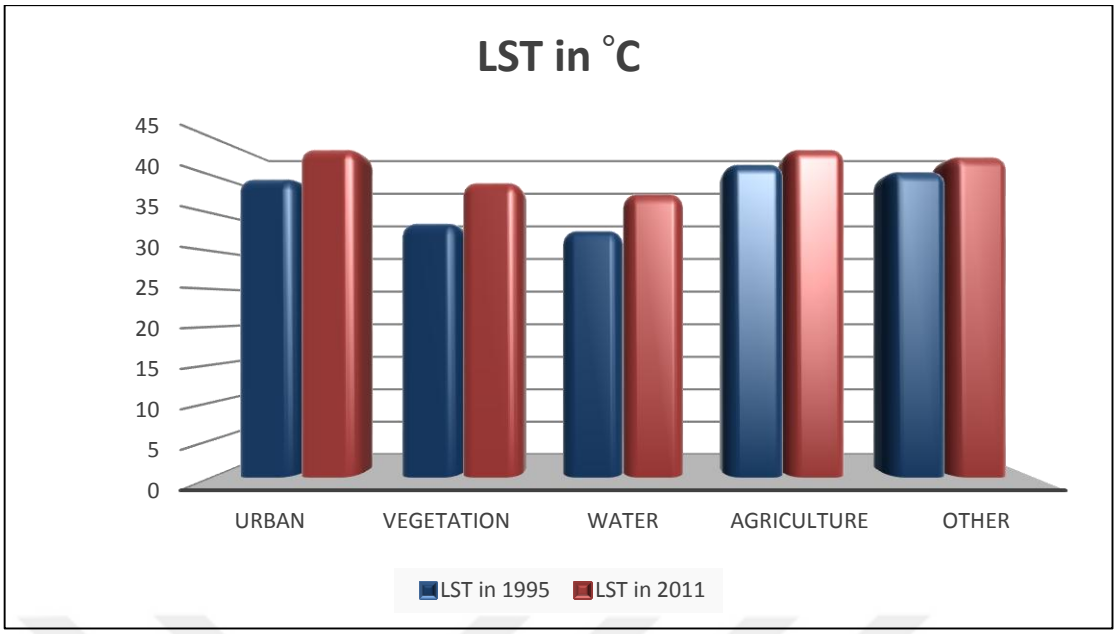

Figure 4.10. A depiction of the mean LST values for the respective land cover classes

4.6. In relation to the correlation between LST outcomes and NDVI

From the existing literature, it is evident that vegetation forms a critical indicator responsible for controlling LST outcomes (Honjo et al., 2004; Ahmed et al., 2005; Habib 2007; Bounoua et al., 2009; Saleh, 2011 and Kumar et al., 2012). In this study, the normalization of NDVI mapping assumed the range -1<=NDVI<=1. Whereas the positive values aided in depicting reflective or vegetated surfaces, negative values depicted the presence of non-reflective, non-vegetative, and water surfaces. Figure 4.9 shows the NDVI map for the study area for both years below concern.

Upon NDVI value extraction, this study revealed a significant change in the nature of vegetation cover. Specifically, vegetation cover and agriculture indicated a general decline from 21.8 % to 13.17 %, the former representing the 1995 outcomes and the latter highlighting the 2011 outcomes. Therefore, greener spaces depicted the highest NDVI values while barren land surfaces were associated with the lowest NDVI values. Water surfaces and urban lands were also associated with the lowest NDVI values, an attribute that was linked to the practice of urban expansion.

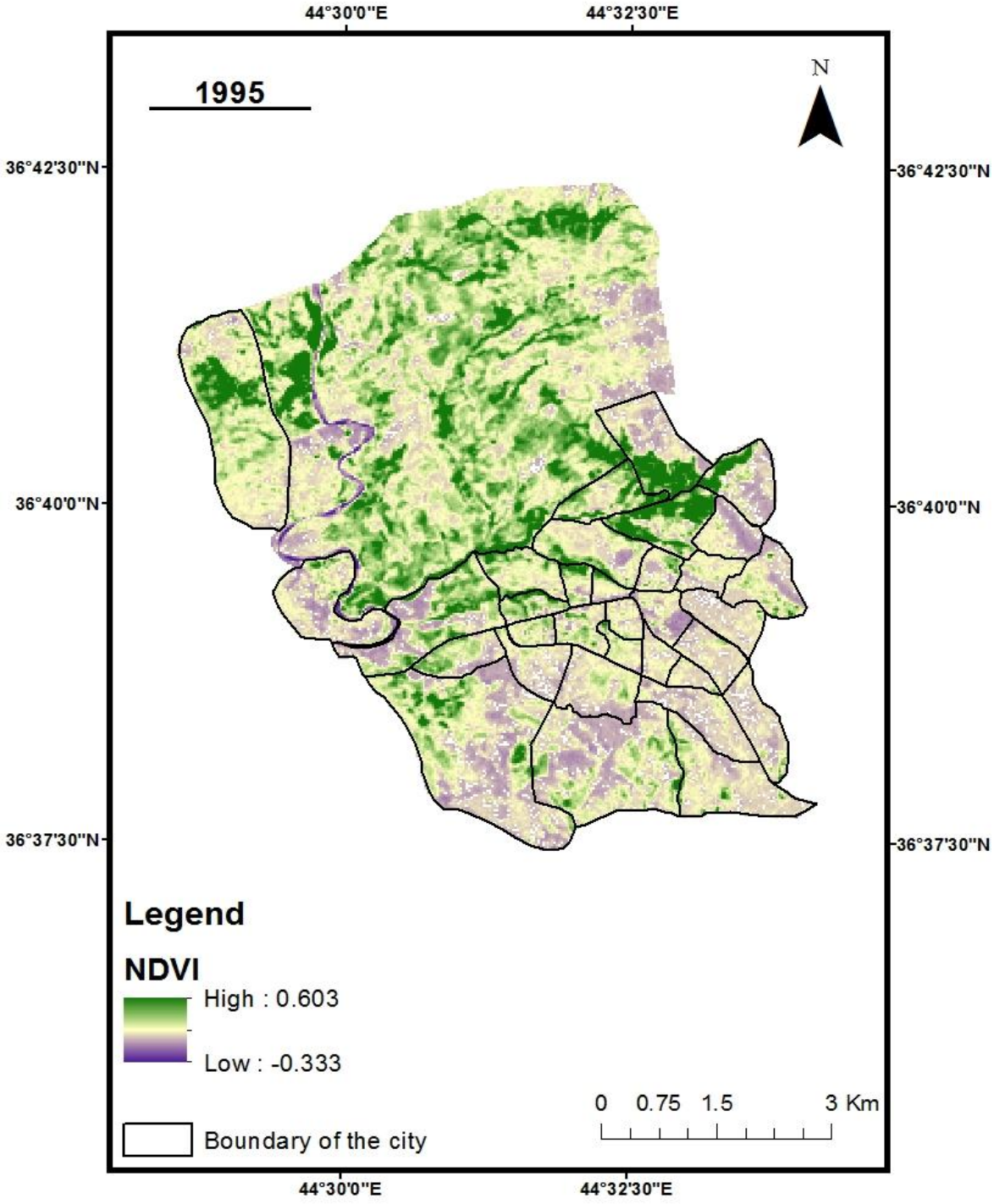

Figure 4.11. NDVI map for 1995

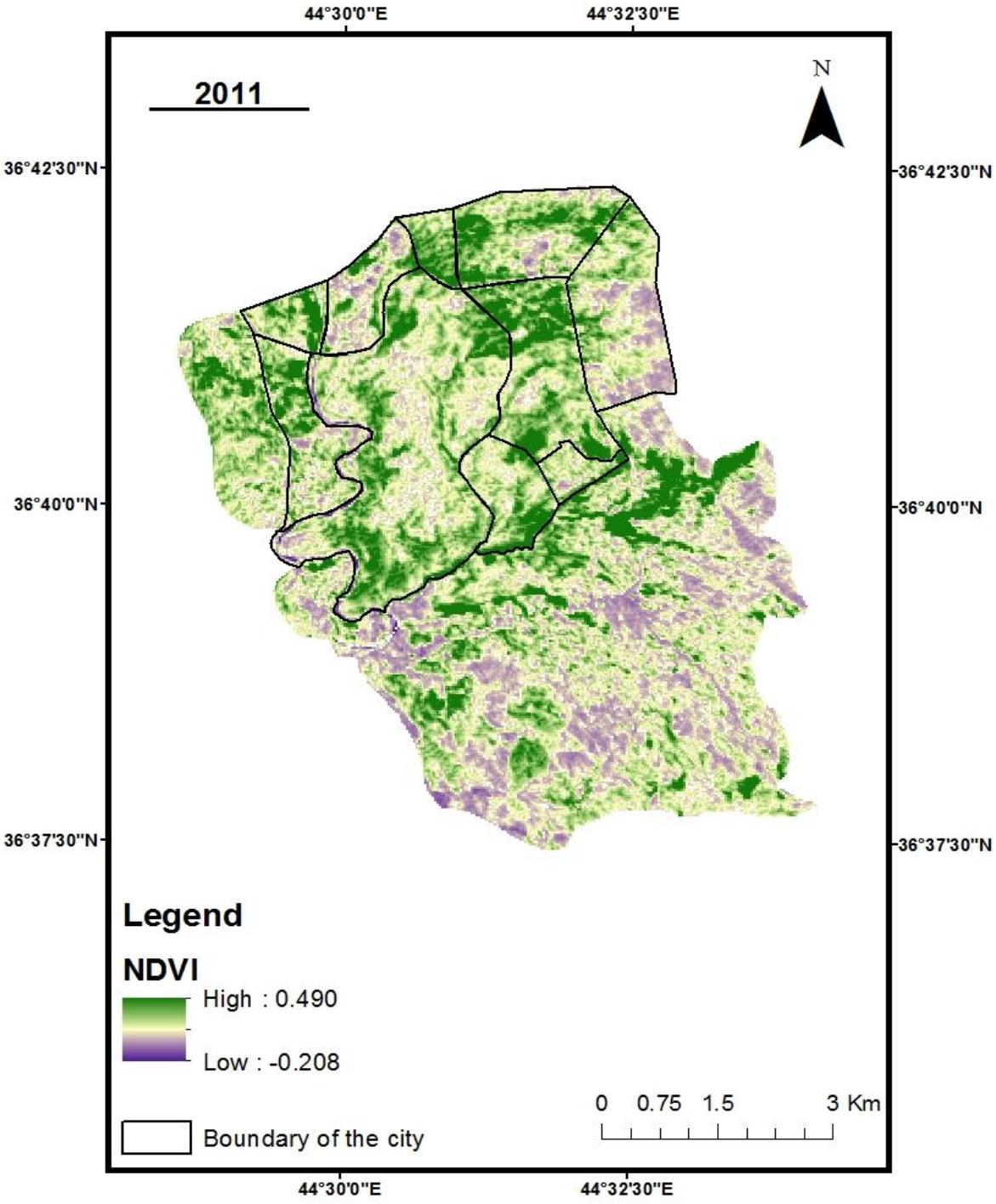

Figure 4.12. NDVI map for 2011

To determine the actual nature of relationship between vegetation cover and LST value outcomes, the Pearson's coefficient analysis was adopted. The relationship between NDVI and LST was also established by employing the linear regression analysis see Figures

4.11 and 4.12. For each image, similar coordinates for NDVI and LST were established and 40 random points selected separately see Tables 4.5 and 4.6.

From the findings of the Pearson correlation coefficient analysis, NDVI and LST values exhibited a strongly negative correlation, for example the correlation result in 1995 is -0.81, and in 2011 it is -0.78. Hence, the outcomes concurred with the findings established by (Honjo et al., 2004; Ahmed et al., 2005; Habib, 2007; Bounoua et al., 2009; Saleh, 2011; Kumar et al., 2012). The R-squared values were also extracted for purposes of determining the degree to which variations in LST were likely to be predicted by NDVI values. Whereas the R-squared outcomes for the year 2011 revealed a value of 0.61, outcomes for the year 1995 revealed a value of 0.65. Indeed, these values are highly significant and suggest that NDVI plays an important role in shaping LST outcomes. This inference is informed by the strongly negative correlation that this study established regarding the relationship between LST and NDVI. Therefore, vegetation cover is important and determines the nature of LST of a given region. The implication is that an increase in NDVI value leads to a significant decrease in the LST value while a decrease in the value of the former yields an increase in the value of the latter. The following Figures 4.13 and 4.14 illustrate a summary of this study's outcomes regarding the correlation between LST values and NDVI outcomes while seeking to examine the impact of urban expansion on LST outcomes in the context of Soran-Erbil.

Table 4.5. Collected values from NDVI and LST maps for 1995

ID	X	Y	NDVI	LST
1	456106.8739	4058247.791	0.093	43
2	453866.1000	4058076.885	0.059	46
3	460018.7335	4058019.916	0.380	32
4	457834.9284	4057773.051	0.223	36
5	459847.8270	4057678.103	0.100	39
6	459354.0972	4056633.674	0.068	41
7	460398.5257	4056215.903	0.023	44
8	458822.3881	4056234.892	0.048	42
9	460455.4945	4054563.807	0.041	46
10	459638.9413	4054297.952	-0.007	47
11	458955.3154	4053937.150	0.035	45
12	457284.2297	4054278.963	-0.015	41
13	457322.2089	4054013.108	-0.023	43
14	458993.2946	4053956.139	0.049	44
15	455651.1233	4059064.344	-0.077	38
16	455328.2999	4057393.259	-0.064	39
17	459733.8894	4058361.729	0.542	33
18	458993.2946	4057697.092	0.520	34
19	454720.6324	4059880.898	0.442	30
20	459316.1179	4060887.347	-0.039	44
21	459164.2011	4058912.427	-0.004	44
22	458366.6375	4054506.838	-0.039	49
23	457977.8616	4053405.775	-0.014	48
24	457056.3544	4061931.775	0.353	38
25	458822.3881	4062007.734	0.347	38
26	459069.2530	4056766.602	-0.040	42
27	456638.5830	4059140.303	0.338	36
28	457702.0011	4061039.264	0.096	42
29	459752.8790	4056405.799	-0.047	45
30	454796.5908	4058817.479	-0.041	47
31	459183.1907	4061836.827	0.092	41
32	457967.8557	4053424.430	-0.014	48
33	460588.4218	4058760.511	0.299	38
34	458157.7518	4056690.643	0.113	41
35	454891.5389	4059956.856	0.211	32
36	455727.0817	4056728.622	0.289	35
37	460949.2244	4054582.796	-0.006	47
38	458803.3985	4054316.942	-0.021	45
39	456695.5518	4056823.570	0.213	39
40	457265.2401	4055665.204	-0.024	45

Table 4.6. Collected values from NDVI and LST maps for 2011

ID	X	Y	NDVI	LST
1	457143.3753	4061950.739	0.174	42
2	456141.4125	4061818.405	0.011	46
3	458296.5778	4061345.781	0.018	45
4	458825.9167	4060476.153	-0.013	48
5	456992.1357	4060797.537	0.065	44
6	455177.2596	4060684.107	0.031	43
7	456027.9828	4058528.942	0.021	45
8	456448.6869	4055608.235	-0.049	47
9	458239.8629	4058150.843	0.071	43
10	456027.9828	4057858.543	-0.006	46
11	455801.1233	4056997.640	0.113	42
12	455158.3547	4056751.876	0.098	42
13	455290.6894	4056732.971	0.189	39
14	456935.4208	4056657.351	0.107	40
15	455990.1729	4056033.487	-0.030	44
16	458126.4332	4055976.772	-0.018	40
17	460243.7886	4056222.537	0.050	40
18	459204.0158	4055901.153	0.018	40
19	460149.2638	4055447.433	0.071	41
20	459033.8712	4054842.475	0.041	43
21	459714.4497	4054634.520	0.054	43
22	459903.4993	4053972.847	0.005	44
23	456569.7211	4054756.829	0.000	44
24	459366.9731	4058657.758	0.198	38
25	457673.3988	4058714.845	0.239	41
26	454931.4952	4060627.392	0.426	37
27	456821.9910	4055371.814	0.375	39
28	460546.2679	4054142.991	0.253	38
29	458504.5324	4061704.975	0.203	41
30	456878.7059	4061894.024	0.341	39
31	458958.2514	4058850.326	0.377	37
32	459317.4456	4057470.264	0.106	39
33	459260.7307	4060816.442	-0.046	48
34	455971.2679	4061667.165	-0.037	47
35	458901.5365	4060967.681	-0.019	49
36	454818.0654	4058869.231	-0.035	46
37	458901.4373	4069873.231	-0.025	50
38	458523.4373	4057791.648	0.068	42
39	455637.3037	4057496.994	0.168	41
40	456500.6067	4057186.690	0.040	45

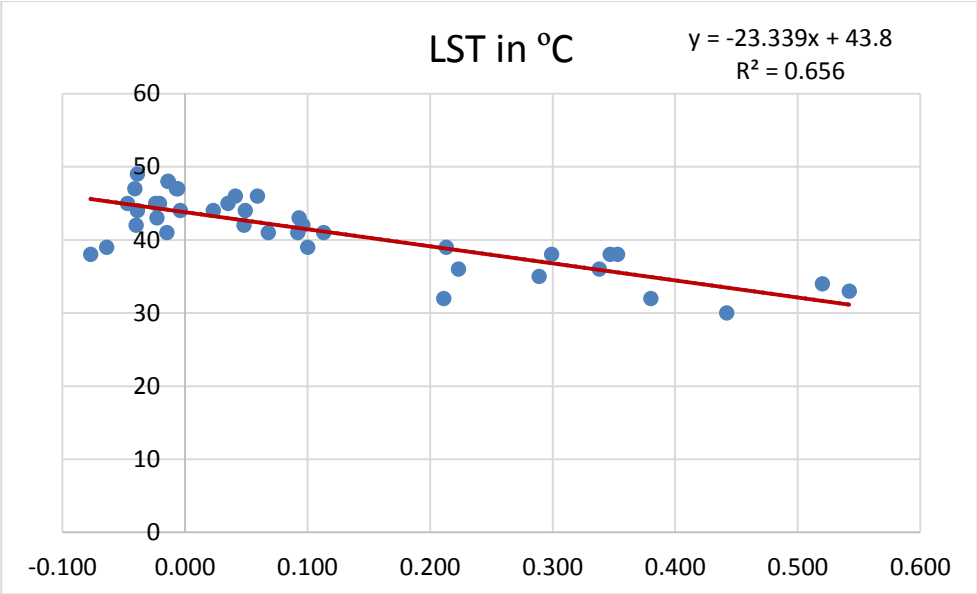

Figure 4.13. Linear regression analysis of outcomes in 1995

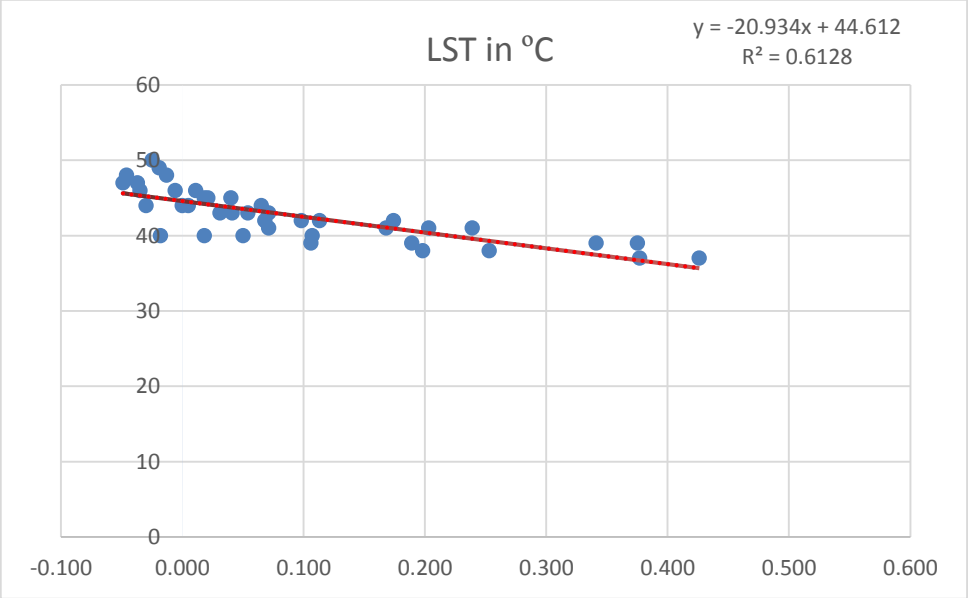

Figure 4.14. Linear regression analysis of outcomes in 2011

5. CONCLUSION

In summary, the central aim of this research was to determine the impact posed by urban expansion on the degree of land surface temperature. Specific insights were gained from the context of Soran-Erbil. It is also worth noting that the study focused on data outcomes for the years 1995 and 2011. Similarly, the GIS system and remote sensing techniques aided in the achievement of the goals and objectives of the research. Indeed, the different land covers were classified with the help of Landsat-5 TM, data, playing an additional role of LST data retrieval for the years 1995 and 2011. The five classes into which land covers were categorized include water, agricultural zones, vegetation, urban zone, and other land. It is further notable that the conversion of digital data into LST values was achieved via the employment of the Radiative Transfer Equation while LST outcome retrieval was conducted via the use of the Landsat thermal band. From the outcomes regarding the classification of the land cover in Soran-Erbil, this study established a significant degree of urban expansion over the 16 year period. At the same time, a significant decline in other land covers was witnessed. With the urban expansion yielding a drastic decline in vegetation cover and the emergence of drought conditions or desertification, the general area is seen to have experienced an increase in the level of LST.

In relation to LST data that is spatially distributed in relation to the districts within and outside the urban zone, this study found that the newly built districts and those that are located around Soran-Erbil had the highest LST temperature in the two years 1995 and 2011. This outcome remained attributable to the decrease in vegetated spaces. Therefore, urban expansion was seen to yield the presence of more open surfaces with the highest surface temperatures in the two years associated with urban and barren lands. Regarding regions where water bodies or accumulations and vegetation were present, the study established that the lowest LST values were associated with such zones. This outcome was linked to the perceived cooling effect on the regions' LST. Thus, it was inferred that water and vegetation constitute critical predictors of LST values. The impact posed by vegetation on the resultant state of LST was also investigated and, after the linear regression and Pearson correlation analyses involving LST outcomes and NDVI values, a strongly negative correlation between the two attributes was established. In summary, it is evident that more valid and reliable outcomes regarding the examination of the impact posed by urban expansion on the LST values are likely to be achieved when the GIS technique is combined with the process of

Landsat thermal band imaging. In Soran-Erbil, it is evident that significant effects of urban expansion on LST have been felt in the recent past and that the need ameliorate these potentially adverse outcomes to the environment cannot be overemphasized, should the relevant authorities strive towards the realization of sustainable development in the wake of a fast-paced urban expansion.

5.1. Suggestions

- With expending of Soran City the government should have a plan for making greener Agriculture and vegetation around the city.
- The people should be helping with government in reducing the usage of those things that would be the reason of increasing LST, such as using Bicycles instead of vehicles and building factories outside the city.
- Because of having many rivers around Soran City, the government should not let this water be wasted by making dams and also having plans for solving the lack of water in which we get benefit agriculturally and climatically.
- Encouraging the private subdivisions to invest in the agricultural lands in the villages and every houses of Soran plain district.
- Building sweatshops and chillers for keeping the products, and transporting the products to the markets.
- The people should avoid cutting the forest and natural trees and keep a live and safe.
- This resulted in correlation and linear regression analyses between NDVI and LST values the analyses show that the strong correlation between NDVI and LST in Soran City is negative, and should have dense vegetation which it has a direct effect on the temperature and NDVI.

REFERENCES

Ahmed, B.M., Hata, T., Tanakamaru, H., Abdelhadi, A.W. and Tada, A. 2005 'Spatial Analysis of Land Surface Temperature and Evapotranspiration for Several Land use/cover Types in the Gezira area, Sudan.' *Koenshu*, 86, 264-265.

Akbari, H., Bell, R., Brazel, T., Cole, D., Estes, M., Heisler, G., and Zalph, B. 2008. *Reducing Urban Heat Islands: Compendium of Strategies Urban Heat Island.* Cengage.

Anderson, J. R. 1976. *A land use and Land Cover Classification System for use with Remote Sensor Data (Vol. 964).* US Government Printing Office.

Armenakis, C., Leduc, F., Cyr, I., Savopol, F., and Cavayas, F. 2003. A ComparativeAnalysis of Scanned Maps and Imagery for Mapping Applications. *ISPRS Journal of Photogrammetry and Remote Sensing*, 57(5), 304-314.

Arnfield, A. J. 2003. Two Decades of Urban Climate Research: a Review of Turbulence, Exchanges of Energy and Water, and the Urban Heat Island. *International Journal of Climatology*, 23(1), 1-26.

Barsi, J. A., Schott, J. R., Palluconi, F. D., and Hook, S. J. 2005 Validation of a Web-Based Atmospheric Correction Tool for Single Thermal Band Iinstruments. In *Optics and Photonics* 2005 (pp. 58820E-58820E). International Society for Optics andPhotonics.

Bhatta, B. 2010. *Analysis of Urban Growth and Sprawl from Remote Sensing Data*. Springer Science and Business Media.

Bounoua, L., Safia, A., Masek, J., Peters-Lidard, C., and Imhoff, M. L. 2009. Impact of Urban Growth on Surface climate: A Case Study in Oran, Algeria. *Journal of applied meteorology and climatology*, 48(2), 217-231.

Campbell, J.B. and Wynne, R.H. 2011. *Introduction to Remote Sensing* (5th Ed.). New York: The guilford press.

Chavez, P. S.1996.Image-Based Atmospheric Corrections-revisited and improved. *Photogrammetric engineering and Remote Sensing, 62(9), 1025-1035.*

Chander, G., and Markham, B. 2003. Revised Landsat-5 TM Radiometric Calibration Procedures and Post Calibration Dynamic Ranges. *Geosciences and Remote Sensing, IEEE Transactions*, 41(11), 2674-2677.

Chander, G., Helder, D. L., and Boncyk, W. C. 2002. Landsat-4/5 Band 6 RelativeRadiometry. Geosciences and Remote Sensing, *IEEE Transactions*, 40(1), 206- 210.

Chuvieco, E. and Huete, A.2010 Fundamental of Satellite Remote Sensing, New York: Taylor and Francis Group.

Congalton, R.G. and Green, K. 2009. *Assessing the Accuracy of Remotely Sensed Data: Principles and Practices (2nd Ed.).* New York: Taylor and Francis Group.

Crist, E. P., and Cicone, R. C. 1984. *A Physically-Based Transformation of Thematic Mapper Data ─ the TM Tasseled Cap.* Geoscience and Remote Sensing, IEEE

Frey, C.M., Rigo, G. and Parlow, E. 2005. '*The Cooling Effect of Cities in a Hot and Dry Environment', Global Developments in Environmental Earth Observation from Space.* Proceedings of the 25th EARSeL Symposium, Porto, Portugal, 169-174.

Gao, J. 2009. *Digital Analysis of Remotely Sensed Imagery*. New York: McGraw – Hill Companies, Inc.

Gartland, L. 2008. Heat Islands: Understanding and Mitigating Heat in Urban Areas. London: Earth scan.

Gillespie, A., Rokugawa, S., Matsunaga, T., Cothern, J. S., Hook, S., and Kahle, A. B. 1998. A Temperature and Emissivity Separation Algorithm for Advanced Spaceborne

Thermal Emission and Reflection Radiometer (ASTER) images. Geoscience and Remote Sensing. *IEEE Transactions*, 36(4), 1113-1126.

Grimond, C. S. B. 2005. Progress in Measuring and Observing the Urban Atmosphere. Theoretical and Applied Climatology, 84(1-3), 3-22.

Habib, B.M. (2007) Islands thermal city of Dammam, a study using the technique of remote sensing and geographic information systems 5 May 2012.

Healey, S. P., Cohen, W. B., Zhiqiang, Y., and Krankina, O. N. 2005. Comparison of Tasseled Cap-Based Landsat Data Structures for use in Forest DisturbanceDetection. *Remote Sensing of Environment*, 97(3), 301-310.

Honjo, T., Ueda, H., Nagatani, Y., Lim, E. and Umeki, K. 2004. 'Analysis of Surface Temperature of Urban Green Spaces by using LANDSAT TM and ETM+data.' *Environmental Information Science*, 259-264.

H.J.Abdullah2012. *The Use of Landsat-5 TM Imagery to Detect Urban Expansion and Its Impact on Land Surface Temperatures in the City of Erbil, Iraq.* Unpublished Master thesis, University of Leicester, UK, Leicester.

Huang, C., Wylie, B., Yang, L., Homer, C., and Zylstra, G. 2002. Derivation of a Tasseled Cap Transformation Based on Landsat 7 at-Satellites Reflectance. *International Journal of Remote Sensing*, 23(8), 1741-1748.

Hodgson, M, E., Jensen, J., Raber, O., Tullis, T, Davis, B, A., Thompson, G., and Schuckman, K. 2005 .An Evaluation of Lidar-derived Elevation and Terrain Slope in Leaf-off Conditions .*Photogrammetric Engineering & Remote Sensing* 823.

Ifatimehin, O. O. 2007. An Assessment of Urban Heat Island of Lokoja Town and Surroundings Using Landsat ETM data. *FUTY Journal of the Environment*, 2(1), 100-108.

Jiménez-Muñoz, J. C., and Sobrino, J. A. 2003. A Generalized Single-Channel Method for Retrieving Land Surface Temperature from Remote Sensing Data. *Journal of Geophysical Research: Atmospheres (1984–2012),* 108, 22.

Jin, M., and Dickinson, R. E.1999. Interpolation of Surface Radiative Temperature Measured from Polar Orbiting Satellites to a Diurnal cycle: 1. Without Clouds. *Journal of Geophysical Research: Atmospheres (1984–2012),* 104(2), 2105-2116.

Kerr, Y.H., Lagouarde, P.J., Nerry, F. and Ottle, C. 2005. 'Land Surface Temperature Retrieval Techniques and Applications: Case of the AVHRR', in Quattrochi, D.A. and Luvall, J.C. (ed.) *Thermal Remote Sensing in Land Surface Processes*, New York: CRC PRESS.

Kiage, L. M., Liu, K. B., Walker, N. D., Lam, N., and Huh, O. K.2007. Recent Land Cover/use Change Associated with Land Degradation in the Lake Baringo Catchment, Kenya, East Africa: Evidence from Landsat TM and ETM+. *International Journal of Remote Sensing,* 28(19), 4285-4309.

Kumar, K. S., Bhaskar, P. U., and Padmakumari, K. 2012. Estimation of Land Surface Temperature to Study Urban Heat Island Effect using Landsat ETM+ Image. *International Journal of Engineering Science and Technology*, 4(2), 771-778.

Kwarteng, A. Y., and Small, C. 2005. *Comparative Analysis of Thermal Environments in New York City and Kuwait City. Proceedings, Remote Sensing of Urban Areas (URS 2005).* Tempe, Arizona, USA, March, 14-16.

Lillesand T.M., Kiefer R.W., 1994. *Remote Sensing and Image Interpretation – A Textbook* (3rd Ed.). Wiley. New York.

Lillesand, T.M., Kiefer, R.W. and Chipman, J.W. 2008. *Remote Sensing and Image Interpretation* (6th Ed.). 111 River Street, Hoboken: NJ: John Wiley and Sons, Inc.

Mahmood, K. W. 2007, Modeling of Soran City Urban Expansion Using Technology of Geographical Information Systems, *ZANCO Journal of Humanity Sciences, Erbil, Iraq*, Vol.(21), No.(1), pp. 148-166.

Markham B.L., Barker J.L., 1986. *Landsat MSS and TM Post-Calibration Dynamic Ranges, ExoatmosphericReflectances and At-Satellite Temperatures.* Earth Observation Satellite Co., Lanham, MD, Landsat Tech. Note 1, Aug.

Mather, P.M. 2004. *Computer Processing of Remotely-Sensed Images* (3rd Ed.). Chichester: John Wiley and Sons, Ltd.

Mallick, J., Kant, Y., & Bharath, B. D. 2008. Estimation of Land Surface Temperature Over Delhi using Landsat-7 ETM+. *J Indian Geophys Union*, 12(3), 131-140.

Mills, G. 2007. Luke Howard, Tim Oke and the Study of Urban Climates. *Weather*, 63, 153-157.

Nichol, J. E. 1994. A GIS-based Approach to Microclimate Monitoring in Singapore's High-Rise Housing Estates. *Photogrammetric Engineering and Remote Sensing*, 60(10), 1225-1232.

Oguz, H. 2013. LST Calculator: a Program for Retrieving Land Surface Temperature from Landsat TM/ETM+ imagery. *Environmental Engineering and Management Journal*, 12(3), 549-555.

Oke, T. R. 1988. The Urban Energy Balance. *Progress in Physical Geography*, 12(4), 471-508.

Oluseyi, I. O., Danlami, M. S., and Olusegun, A. J. 2011. Managing Land Use Transformation and Land Surface Temperature Change in Anyigba Town, Kogi State, Nigeria. *Journal of Geography and Geology*, 3(1), 77.

Prakash, A. 2000. Thermal Remote Sensing: Concepts, Issues and Applications. *International Archives of Photogrammetric and Remote Sensing*, 33, 239-243.

Prigent, C., Aires, F., and Rossow, W. B. 2003. Land Surface Skin Temperatures from a Combined Analysis of Microwave and Infrared Satellite Observations for an all Weather Evaluation of the Differences Between air and Skin Temperatures. *Journal of Geophysical Research: Atmospheres (1984–2012),* 108, 10.

Qin, Z. H., Karnieli, A., and Berliner, P. 2001. A Mono-Window Algorithm for Retrieving Land Surface Temperature from Landsat TM Data and its Application to the Israel-Egypt Border Region. *International Journal of Remote Sensing*, 22(18), 3719-3746.

Rajeshwari, A., and Mani, N. D. Estimation of Land Surface Temperature of Din Digul districts using Landsat 8 Data. International Journal of Research in Engineering and Technology, 3(05), 122-126.

Rizwan, A. M., Dennis, L. Y., and Chunho, L. I. U. 2008. A Review on the Generation, Determination and Mitigation of Urban Heat Island. *Journal of Environmental Sciences*, 20(1), 120-128.

Saleh, S. A. 2011. Impact of Urban Expansion on Surface Temperature in Baghdad, Iraq using remote sensing and GIS techniques. *Canadian Journal on Environmental, Construction and Civil Engineering*, 2(8), 193-202.

Singh, A., Singh, S., Garga, P. K., and Khanduri, K. 2013. Land Use and Land Cover Change Detection: A Comparative Approach Using Post Classification Change Matrix and Discriminate Function Change Detection Methodology of Allahabad City. *International Journal of Current Engineering and Technology*, 2277- 4106.

Snyder, W. C., Wan, Z., Zhang, Y., and Feng, Y. Z. 1995. Classification-Based Emissivity for Land Surface Temperature Measurement from Space. *International Journal of Remote Sensing*, 19(14), 2753-2774.

Sobrino, J. A., Jimenez Munoz, J. C., and Paolini, L. 2004. Land Surface Temperature Retrieval from LANDSAT TM 5. *Remote Sensing of Environment*, 90(4), 434-440.

Sobrino, J. A., Jiménez-Muñoz, J. C., Sòria, G., Romaguera, M., Guanter, L., Moreno, J. and Martinez, P. (2008). Land Surface Emissivity Retrieval from Different VNIR and TIR sensors. *IEEE Transactions on Geosciences and Remote Sensing, 46(2), 316-327.*

Sun, D., and Pinker, R. T. 2003. Estimation of Land Surface Temperature from a Geostationary Operational Environmental Satellite (GOES8). *Journal of Geophysical Research: Atmospheres (1984–2012), 108, 11*.

Tanriverdi, C., 2010. Improved Agricultural Management Using Remote Sensing To Estimate Water Stress Indices. Appl Rem Sens Journal 1(2):19-24.

Tanriverdi, C. 2003. Available water effects on water stress indices for irrigated corn grown in sandy soils. Ph. D. Thesis, Department of Chemical and Bioresource Engineering, Colorado State University, Fall 2003.

Thorne, K., Markharn, B., Barker,P.S., and Biggar, S.1997. Radiometric Calibration of Landsat. *Photogrammetric Engineering and Remote Sensing*, 63(7), 853-858.

Tso, B. and Mather, P.M. 2009. *Classification Methods for Remotely Sensed Data* (2nd Ed.). New York: Taylor and Francis Group

Voogt, J. A. and Oke, T. R. 2003. Thermal Remote Sensing of Urban Climates. *Remote sensing of environment*, 86(3), 370-384.

Wan, Z., and Dozier, J. 1996. A Generalized Split-Window Algorithm for Retrieving Land-Surface Temperature from Space. *Geoscience and Remote Sensing, IEEE Transactions*, 34(4), 892-905.

Watson, K. 1992. Spectral Ratio Method for Measuring Emissivity. *Remote Sensing of Environment*, 42(2), 113-116.

Weng, Q., Lu, D., and Schubring, J. 2004. Estimation of Land Surface Temperature-Vegetation Abundance Relationship for Urban Heat Island Explorations. *Remote sensing of Environment,* 89(4), 467-483.

Zhang, J., Wang, Y., and Li, Y. 2006. A C++ Program for Retrieving Land Surface Temperature from the Data of Landsat TM/ETM+ Band6. *Computers and Geosciences*, 32(10), 1796-1805.

Zhang, Q. and Ban, Y. 2011. Evaluation of Urban Expansion and Its Impact on Surface Temperature in Beijing, China. *Journal ofUrban Remote Sensing Event (JURSE),* 357-360.

CURRICULUM VITAE

Personal Identity

Name, Surname	Chiya Sami Suliaman BAG
Nationality	Iraqi
Date and place of birth	05. December. 1989, Soran , Erbil, Iraq
Marital Status	Married
Telephone	+964 750 451 2989
E-mail	Chiya_soran@yahoo.com

Educational Background

degree	Place of Education	Date of graduate
High school	Shahid Abdulrahman High School	2002 - 2007
Bachelor's degree	Soran University, Faculty of Education ,Geographic department	2008 - 2011
Master degree	Graduate School of Nature, Dep. of Bioengineering and Applied Science, Kahramanmaraş sütçü imam University, Turkey	2015 - 2018

Knowledge of Language:

Kurdish: Mother language.

Turkish: read & write & speak

English: read & write & speak.

Arabic: read & write & speak.

Persian: read & speak.

Publications:

- Çağatay TANRIVERDİ, Chiya SAMI, Engin GONEN, Determining thermal comfort zones for outdoor recreation A case study of Shaqlawa – Erbil - Iraq, The 4th International Geography Symposium , 23-26 May 2016 , Kemer – Antalya – TUTKEY . PP: 338.